Complete set of homogeneous isotropic analytic solutions in scalar-tensor cosmology with radiation and curvature

Itzhak Bars, Shih-Hung Chen, Paul J. Steinhardt, and Neil Turok

Phys. Rev. D **86**, 083542 — Published 26 October 2012

DOI: 10.1103/PhysRevD.86.083542

Complete Set of Homogeneous Isotropic Analytic Solutions in Scalar-Tensor Cosmology with Radiation and Curvature

Itzhak Bars[*], **Shih-Hung Chen**[†], **Paul J. Steinhardt**[#] **and Neil Turok**[†]

[*] *Department of Physics, University of Southern California, Los Angeles, CA 90089, USA*

[†] *Perimeter Institute for Theoretical Physics, Waterloo, ON N2L 2Y5, Canada*

[#] *Department of Physics and Princeton Center for Theoretical Physics*

Princeton University, Princeton, NJ 08544, USA

Abstract

We study a model of a scalar field minimally coupled to gravity, with a specific potential energy for the scalar field, and include curvature and radiation as two additional parameters. Our goal is to obtain analytically the complete set of configurations of a homogeneous and isotropic universe as a function of time. This leads to a geodesically complete description of the universe, including the passage through the cosmological singularities, at the classical level. We give all the solutions analytically without any restrictions on the parameter space of the model or initial values of the fields. We find that for generic solutions the universe goes through a singular (zero-size) bounce by entering a period of antigravity at each big crunch and exiting from it at the following big bang. This happens cyclically again and again without violating the null energy condition. There is a special subset of geodesically complete non-generic solutions which perform zero-size bounces without ever entering the antigravity regime in all cycles. For these, initial values of the fields are synchronized and quantized but the parameters of the model are not restricted. There is also a subset of spatial curvature-induced solutions that have finite-size bounces in the gravity regime and never enter the antigravity phase. These exist only within a small continuous domain of parameter space without fine tuning initial conditions. To obtain these results, we identified 25 regions of a 6-parameter space in which the complete set of analytic solutions are explicitly obtained.

PACS: 98.80.-k, 98.80.Cq, 04.50.-h.

Keywords: big bang, inflation, cosmology, Weyl symmetry, gravity, antigravity, 2T-physics.

I. INTRODUCTION

Scalar-tensor theory has been one of the most popular tools for building models in cosmology. It is sufficiently simple while having a variety of applications. One common application is to describe early universe inflation [1–3] where the scalar plays a central role in driving a period of accelerated expansion that solves the homogeneity (horizon) and the flatness problems, and generates the primordial density perturbation that seeds the subsequent growth of the large scale structure[4–7]. Alternatively, ekpyrotic [8, 9] and tachyacoustic [10] models for the early universe models also utilize scalar-tensor theories to produce a period of a slow contracting phase before a big crunch that eliminates the horizon problem, and solves the flatness problem as well. With some specific matching rules inspired by a colliding two branes picture, ekpyrotic models can also generate scale invariant density perturbations as observed today. Another application of scalar-tensor theories is to produce the late time acceleration of the universe that is inferred from type IA supernova observations [11]. Such models are called "quintessence" models where a small nonzero dynamical vacuum value of a scalar potential replaces the cosmological constant [12]. In addition, by using a conformal transformation, it has been shown that modified gravity theories, such as $f(R)$ gravity, are equivalent to scalar-tensor theory with a specific scalar potential [13].

Despite such broad applications of scalar-tensor theories, only a few isolated examples of analytic solutions have been found so far. This is because the coupled second order nonlinear differential equations are hard to solve analytically. Our goal in this paper is to provide a full set of analytic solutions that give all possible configurations of a *homogeneous* and *isotropic* universe as a function of time. This expands on our previous work in [14–16] by including additional degrees of freedom, in particular radiation. The effects of anisotropy are discussed elsewhere [17, 18].

Our overall approach in this paper is in contrast to specific analytic, approximate or numerical solutions that are usually fine tuned from the point of view of initial conditions and/or the potential energy function $V(\sigma)$ for the scalar field, to force a solution in which the universe has a particular desired behavior as motivated by prejudices and observations. Instead, we would like to understand the global structure of solution space that can emerge from a class of theories, so that we can gain a better understanding of how the features of our own universe could emerge. Obtaining the full set of classical solutions can provide some such insights. Indeed through our solutions we gain new understanding about general generic behavior as we will see below.

We can obtain the full set of analytic solutions of the scalar-tensor theory for several forms of the potential energy function $V(\sigma)$ for the scalar field. In this paper we concentrate on the case:

$$V(\sigma)=\left(\frac{6}{\kappa^2}\right)^2\left[c\sinh^4\left(\sqrt{\frac{\kappa^2}{6}}\sigma\right)+b\cosh^4\left(\sqrt{\frac{\kappa^2}{6}}\sigma\right)\right], \tag{1}$$

where the parameters b and c are dimensionless free parameters, and κ^{-1} is the reduced Planck mass $\kappa^{-1}=\sqrt{\frac{hc}{8\pi G}}=2.43\times10^{18}\frac{GeV}{c^2}$. We note that this potential has familiar features. For example, if $(b+c)>0$, depending on the various values and signs of b,c, $V(\sigma)$ has a single well or double well with stable minima, similar to other potentials used in cosmological applications. Because our analysis has a broad range of applications beyond cosmology, we will classify all the solutions regardless of the physical application. In other papers, including [17, 18], the role of these solutions is discussed in a cosmological setting. Some of these cases will be pointed out briefly later in the paper. In a separate paper we will present the analytic solutions for the potentials $V(\sigma)=\frac{6^2}{\kappa^4}be^{2p\kappa\sigma/\sqrt{6}}$ for arbitrary p and $V(\sigma)=\frac{6^2}{\kappa^4}\left(be^{-2\kappa\sigma/\sqrt{6}}+ce^{-4\kappa\sigma/\sqrt{6}}\right)$, where b,c,p are dimensionless real parameters.

For the potential 1, we can solve the Friedmann equations exactly for all time intervals before or after the big bang. The method, which is based on conformal symmetry, was introduced in previous papers [14]-[18]. It was applied to the cases of the flat and curved isotropic Friedmann universes without radiation or matter [15]. It was also applied to the case of an anisotropic universe in the absence of the potential energy, but with the inclusion of radiation [18]. In this paper, we further generalize our method for the isotropic universe to include both curvature and radiation with the potential, where radiation is taken in the form of a perfect fluid. The inclusion of radiation is a simple mathematical exercise beyond our previous paper [15], but it describes richer physics, and leads to more complicated analytic expressions for the solutions. So, the reader may wish to first understand the previous work in a simpler setting [15].

Including radiation, the model is defined by 4 parameters, namely (b,c) in the potential, the curvature parameter K in the metric, and ρ_r, the energy density of radiation when the scale factor is $a=1$. The two fields of interest are the time dependent scale factor $a(\tau)$ and the scalar field $\sigma(\tau)$. Their initial conditions $(a(\tau_0),\dot{a}(\tau_0),\sigma(\tau_0),\dot{\sigma}(\tau_0))$ introduce 4 more parameters which enter the general solution to second order. However, the zero energy condition including gravity (or Friedmann equation) eliminates one of the initial values, and one other initial value can be absorbed into a redefinition of the initial time τ_0 by using the time translation symmetry of the differential equations. Hence the complete set of solutions are described by 4+2=6 parameters given by $(b, c, K, \rho_r, E, a(\tau_0))$,where a single energy parameter E is used conveniently instead of the two related initial velocities $\dot{a}(\tau_0), \dot{\sigma}(\tau_0)$. We will give all the analytic solutions without putting any conditions on these 6 parameters at any τ_0. It turns out that there are 25 distinct regions of this parameter space in which the solutions take different analytic forms in terms of Jacobi functions. The 25 regions and the corresponding solutions are given explicitly in the Appendix. If an unstable potential with $(b+c) < 0$ is of interest there would be more regions and corresponding solutions; with appropriate modifications these can be obtained from those available in the Appendix.

As in our previous work [15, 16], we find that in the Einstein frame the generic solutions are geodesically incomplete at the cosmological singularity (see Eqs. (3) and (4) in [15]). We will then find that the knowledge of the full set of solutions suggests how to complete the space and make it geodesically complete for the generic solution. This completion includes time intervals during which the gravitational field effectively acts like a repulsive force (antigravity) rather than an attractive force (gravity). So, the generic solution has alternating time intervals of gravity and antigravity as graphically illustrated in Fig. 2. In this figure, each time the trajectory crosses the 45^o lines, the universe transits from gravity to antigravity or vice-versa. There is however a subset of non-generic solutions that are geodesically complete in the Einstein frame without ever entering the antigravity region. These are of two types: (i) singular zero-size bounces at the cosmic singularity without violating the null energy condition as shown in Fig. 3 and (ii) non-singular finite-size bounces as shown in Figs.(23,24) in [15].

The zero-size bounces (i), which are classified in tables I, IIb and III, with the related analytic expressions in the Appendix, are obtained by synchronizing and/or quantizing some initial values. These tables provide the most general parameter subspace (within the 6-parameter set) for which the geodesically complete singular bounce occurs without antigravity. The parameter subset consists of 4 continuous and one quantized parameter, which is obviously smaller than the available continuous 6-parameter set. Despite the fact that this subset of solutions may be considered a set of measure zero as compared to the full set, it is distinguished as the only zero-size bounce set of solutions that are geodesically complete in the Einstein frame, and do not enter the antigravity region at any time in any cycle.

The finite-size-bounces (ii), which are classified in table IIa, with the related analytic expressions in the Appendix, describe a universe that contracts up to a minimum non-zero size, at which point the spatial curvature causes the universe to bounce back into an expanding phase. This kind of spatial curvature-induced bounce is already familiar in cosmology. Here we provide analytic solutions for the finite-size bounces. As the universe turns around to repeat such cycles, the minimum size is not necessarily the same in each cycle, as this depends on the parameters. Such solutions occur when the parameters satisfy, $\rho_r < K^2/16b$ and $\phi^2_{\min}(\tau_0) > K/4b > s^2_{\max}(\tau_0)$ (see Table IIa). Note that there are still 6 parameters, so this is a continuous set, but it is a restricted region of parameter space or initial values.

The solutions above – the generic case, type (i) or type (ii) bounces – are the exact and complete set of solutions in the absence of anisotropy. Although anisotropy can be neglected as the universe expands, it can grow to be a dominant effect near the singularity. We do not consider those cases here; they are described in [17, 18] where it is proven that there is an attractor mechanism that is independent of initial conditions. The attractor distorts the zero-bounce solutions, both the generic or non-generic type (i), to behave in a unique way such that these solutions must undergo a big crunch/big bang transition by contracting to zero size, passing through a brief antigravity phase, shrinking to zero size again, and re-emerging into an expanding normal gravity phase.

This paper is organized as follows. In Sec. II, we introduce the standard scalar-tensor theory, with a single minimally coupled scalar field $\sigma(x)$, as the gauge fixed version of a locally scale (Weyl) invariant reformulation of Einstein's theory of gravity that contains two conformally coupled scalar fields $\phi(x), s(x)$. This "Weyl lifted" version has an extra scalar field as well as a local Weyl symmetry that compensate each other, so that the physical degrees of freedom are the same number as in the standard formulation of the theory. This model and method of solution emerged directly from the 2T-physics formulation of gravity [19–21]. The model was also inspired in the context of braneworld notions [22, 23] that led to the colliding brane scenario for cosmology [8, 9, 24, 25]. Recently 'tHooft also motivated the same Weyl invariant theory because of its ability to give a better description of black and white holes in a convenient gauge [26]. Such gauge choices, including the E, γ, c and

s gauges discussed in this paper, are just a small subset of examples of 3+1 dimensional "shadows" that 2T-physics yields as dual forms of the same parent theory that unifies them in 4+2 dimensions.

The Weyl lifted version has no dimensionful constants, not even the gravitational constant. The extra scalar field can be eliminated by gauge fixing it to a dimensionful constant, thus reaching what we call the "Einstein gauge" (E-gauge), the standard formulation of the theory in the Einstein frame with the usual gravitational constant and the scalar field σ. The advantage of the Weyl lifted version is that it allows us to choose another more convenient gauge that we call the γ-gauge, in which the cosmological equations greatly simplify and can be solved analytically. The full set of solutions is then mapped to the Einstein frame by a gauge transformation from the γ-gauge to the E-gauge, and verified that they are the solutions of the Friedmann equations. In this process we only add gauge degrees of freedom to Einstein's theory. But in the presence of the gauge degrees of freedom we find naturally the geodesically complete space and understand much more clearly the nature of the complete space of solutions. In particular we learn that geodesic completeness requires an extension of the domain of the original fields in the scalar-tensor theory in the Einstein frame, such that with this extension, the same fields can describe also an antigravity region not captured at first sight.

In Sec. III we show how the complete set of solutions of the Friedmann equations, including curvature and radiation, are obtained analytically without constraining the 6-parameter space. The complete set of solutions is explicitly given in the Appendix, where in 25 different regions of the parameter space the analytic expressions take different forms. These solutions are all cyclic and geodesically complete in an enlarged domain as described above.

The non-generic solutions of type (i) with zero-size bounces, and type (ii) with finite-size bounces, which never enter the antigravity regime, are still geodesically complete in the gravity domain. In Sec. IV we determine the constraints on parameter space and initial conditions that distinguish the geodesically complete solutions in the restricted Einstein frame. The corresponding parameter spaces are classified in Tables I, IIa,b and III.

In Sec. V we comment on the generic solutions that are geodesically complete provided an anti-gravity regime is included.

In Sec. VI we summarize our results. In an Appendix (A) we list all the analytic cosmological solutions predicted by our model introduced in Sec. II.

II. THE WEYL LIFTED MODEL

Our approach begins with the standard action typically used in cosmological models that describe a scalar field $\sigma(x^\mu)$ minimally coupled to gravity

$$S_{gravity} = \int d^4x\sqrt{-g_E}\left\{\begin{array}{c}\frac{1}{2\kappa^2}R\left(g_E\right) - \frac{1}{2}g_E^{\mu\nu}\partial_\mu\sigma\partial_\nu\sigma - V\left(\sigma\right) \\ +radiation + matter,\end{array}\right\}. \tag{2}$$

where the subscript E refers to the Einstein (E-)gauge (see below). We are able to solve for the complete set of homogeneous, isotropic, cosmological solutions of this model when the potential $V(\sigma)$ is given as in Eq. (1). Through these solutions we discover the geodesic completion of the space through the cosmological singularity.

To solve the equations and to understand the geodesic completion we will use a device that we call "Weyl extension" in which the model is enlarged by adding gauge degrees of freedom that are compensated with a local scaling (Weyl) symmetry. The local scaling symmetry does not allow the usual Einstein-Hilbert term $R(g_E)/2\kappa^2$, but allows conformally coupled scalars. The following action, which will be shown to be related to the one above by a gauge choice, contains two conformally coupled scalars, ϕ, s, interacting with the curvature term with the coefficient $\frac{1}{12}$ dictated by the gauge symmetry

$$S = \int d^4x\sqrt{-g}\left(\frac{1}{2}g^{\mu\nu}\partial_\mu\phi\partial_\nu\phi - \frac{1}{2}g^{\mu\nu}\partial_\mu s\partial_\nu s + \frac{1}{12}\left(\phi^2 - s^2\right)R\left(g\right) - \phi^4 f\left(\frac{s}{\phi}\right)\right). \tag{3}$$

The function $f(z)$ is determined by the scalar field potential (see below) and, in general, can be an arbitrary function of the gauge invariant ratio $z \equiv \frac{s}{\phi}$ and still maintain the Weyl symmetry. The metric $g_{\mu\nu}$ can differ from the metric $g_{\mu\nu}^E$ in Eq. (2) by an arbitrary conformal factor because of the gauge symmetry under the following local transformation

$$\phi \to \Omega\phi,\ s \to \Omega s,\ g_{\mu\nu} \to \Omega^{-2}g_{\mu\nu},$$

where $\Omega(x)$ is an arbitrary function of spacetime. (Note the the metric here undergoes a field re-scaling rather than a coordinate transformation.)

This action was described as the *conformal shadow* of the 2T-Gravity action [20, 21] in 4+2 dimensions. In this setting, it was shown that the local scaling gauge symmetry is a remnant of general coordinate transformations in the extra 1+1 dimensions.

We draw attention to the fact that ϕ has the wrong sign kinetic term while s has the correct sign. It appears as if ϕ is a ghost; however, since the ghost disappears for some choices of gauge (e.g. the gauge that restores the Einstein gravity form of the theory), there is no real problem with ghosts or unitarity. In this connection, note also that there is no gravitational constant; rather, the factor $\frac{1}{12}\left(\phi^2 - s^2\right)$ effectively behaves like a gravitational parameter which replaces the usual expression $(16\pi G)^{-1} = \left(2\kappa^2\right)^{-1}$ where G is the Newton constant. If ϕ had the opposite sign kinetic term, then this factor would become purely negative $\frac{1}{12}\left(-\phi^2 - s^2\right)$ in order to maintain the Weyl symmetry, but then the gravitational parameter would have the wrong sign. This is the reason why ϕ must be introduced initially with the "wrong" sign, so that the gravitational parameter $\frac{1}{12}\left(\phi^2 - s^2\right)$ is positive at least in some regions of field space.

Fermionic and gauge fields, as well as more conformally coupled scalars, can be added, to construct a completely Weyl invariant model, such as the Standard Model of particle physics. The Higgs field must also couple as a conformal scalar to preserve the Weyl symmetry. The Higgs mass term is not allowed by the gauge symmetry, but it can be generated by coupling the Higgs doublet H to the singlets ϕ, s in Weyl invariant quartic terms of the form $H^\dagger H\left(\alpha\phi^2 + \beta s^2\right)$. There are various possible models for the effective Higgs mass by choosing the parameters α, β. One possibility is related to the fact that $\left(\phi_E^2 - s_E^2\right)$ gets fixed to a constant in the Einstein gauge of Eq. (6). Another possibility emerges from our solutions, by noting that cosmologically $s_E = \frac{\sqrt{6}}{\kappa}\sinh\left(\frac{\kappa\sigma(\tau)}{\sqrt{6}}\right)$ evolves to a field $s_E \sim \sigma(\tau)$ which is much smaller than the Planck scale, and at late times behaves almost like a constant that can mimic the Higgs mass term. This might also explain the mass hierarchy [27, 28].

We discuss here four gauge choices that are useful for finding solutions and interpreting them: Einstein gauge (E-gauge), the γ-gauge, the supergravity gauge (c-gauge) and the string gauge (s-gauge). To distinguish the fields in each gauge we denote them by the subscripts E, γ, c, s respectively. We also define the following Weyl gauge invariant quantity χ which plays an important role in our discussion

$$\chi \equiv \frac{\kappa^2}{6}(-g)^{\frac{1}{4}}(\phi^2 - s^2). \tag{4}$$

Another gauge invariant is the ratio s/ϕ.

E-gauge: The usual Einstein gravity in Eq. (2) is obtained in the E-gauge, in which we denote the fields by $\phi_E(x), s_E(x), g_E^{\mu\nu}(x)$ with a subscript E. In this gauge the gravitational parameter is gauge fixed to the usual Newton constant for all spacetime x^μ

$$\frac{1}{12}\left(\phi_E^2(x) - s_E^2(x)\right) = \left(2\kappa^2\right)^{-1}. \tag{5}$$

Then parameterizing this gauge with a single scalar field σ,

$$\phi_E(x) = \pm\frac{\sqrt{6}}{\kappa}\cosh\left(\frac{\kappa\sigma(x)}{\sqrt{6}}\right),\ s_E(x) = \pm\frac{\sqrt{6}}{\kappa}\sinh\left(\frac{\kappa\sigma(x)}{\sqrt{6}}\right), \tag{6}$$

we find that the conformally gauge invariant action (3) yields the familiar action in Eq. (2) with an Einstein-Hilbert term $\frac{1}{2\kappa^2}R(g_E)$ and a minimally coupled scalar field σ, just as in Eq. (2). The gauge invariant χ in the E-gauge becomes

$$\chi = (-g_E)^{\frac{1}{4}}. \tag{7}$$

In a cosmological solution with the metric

$$ds_E^2 = a_E^2(\tau)\left(-d\tau^2 + ds_3^2\right) \tag{8}$$

where the 3-dimensional metric ds_3^2 will be discussed later, $(-g_E)^{\frac{1}{4}}$ is just the scale factor of the universe, $\chi = a_E^2(\tau)$, so χ must vanish at the cosmological singularity at the time of the big bang $a_E(\tau_B) = 0$. This shows that the big bang corresponds to $\chi(\tau_B) = 0$, and since χ is gauge invariant, the cosmological singularity is at $\chi(\tau_B) = 0$ in all gauges.

Note that the geometry completely collapses at the singularity at time τ_B in the E-gauge since $(-g_E(\tau_B)) = 0$, and this is why geodesics are incomplete. However, we will see that the geometry does not collapse at all at $\chi(\tau_B) = 0$ in the other gauges, and this is how we are able to complete the geodesics and the geometry.

γ-gauge: In the γ-gauge we choose $(-g_\gamma)^{\frac{1}{4}}$=constant for all τ. Since the cosmological FRW metric in the E-gauge is conformally flat (even when the curvature is non-zero), $ds_E^2 = a_E^2(\tau)(-e^2d\tau^2 - ds_{3FRW}^2)$, we can at first discuss the *general conformally flat metric* which can always be put into the form $ds^2 = a^2(x^\mu)\eta_{\mu\nu}$, where $\eta_{\mu\nu}$ is the Minkowski metric. A conformally flat metric becomes fully flat in the γ-gauge $ds^2 = \eta_{\mu\nu}$, namely the gauge choice $a_\gamma(x) = 1$, leading to $R(g_\gamma) = 0$. Hence the degrees of freedom in the γ-gauge are ϕ_γ, s_γ in a flat Minkowski geometry. The gauge invariant χ now takes the form

$$\chi(x^\mu) = \frac{\kappa^2}{6}(\phi_\gamma^2 - s_\gamma^2)(x^\mu), \tag{9}$$

and the gauge invariant action in (3), taken with any conformally flat metric, reduces to a gauge fixed action in flat Minkowski space

$$S_\gamma = \int d^4x\left[\frac{1}{2}\left((\partial_\mu\phi_\gamma)^2 - (\partial_\mu s_\gamma)^2\right) - \phi_\gamma^4 f\left(\frac{s_\gamma}{\phi_\gamma}\right)\right], \tag{10}$$

where $\phi_\gamma(x)$ is a ghost since it has the wrong-sign kinetic energy. However, this ghost is removed as follows: before choosing the γ-gauge we recall that there was an Einstein equation for the metric, $G_{\mu\nu}(g) = T_{\mu\nu}$, which must be imposed for any metric in the γ-gauge as well. For the conformally flat metric in the present case, the curvature vanishes in the γ-gauge, $R_{\mu\nu\lambda\sigma}(\eta) = 0$, leading to $G_{\mu\nu}(\eta) = 0$, and therefore $T_{\mu\nu}(\phi_\gamma, s_\gamma) = 0$. The vanishing of the stress tensor for the action S_γ is a constraint that removes the ghost ϕ_γ.

To include the effect of both anisotropy and curvature, the 3-dimensional part of the FRW metric, $(ds_3^2)_{FRW}$, must be replaced by the corresponding 3-dimensional parts of the Kasner metric, Bianchi IX metric, Bianchi VIII metric, when $K = 0$, $K > 0$, $K < 0$ respectively. We parameterize the Kasner metric ($K = 0$) as follows

$$\left(ds_3^2\right)_{Kasner} = e^{-2\sqrt{2/3}\kappa\alpha_1}(dz)^2 + e^{\sqrt{2/3}\kappa\alpha_1}\left(e^{\sqrt{2}\kappa\alpha_2}(dx)^2 + e^{-\sqrt{2}\kappa\alpha_2}(dy)^2\right),$$

where $\alpha_1(x^\mu)$ and $\alpha_2(x^\mu)$ are the anisotropy fields that are taken to depend only on time in the homogeneous case considered in this paper. The Bianchi IX and VIII metrics contain the same $\alpha_{1,2}(x^\mu)$, as well as the non-zero curvature parameter K that is included by generalizing (dx, dy, dz) to $(d\sigma_x, d\sigma_y, d\sigma_z)$. Both of these Bianchi metrics reduce to the Kasner metric when the curvature K vanishes.

In the homogeneous limit, with an anisotropic cosmological metric of the form given above, $ds^2 = a^2(\tau)\left(-e^2 d\tau^2 - ds_3^2\right)$, the Weyl invariant action reduces to the following effective action for the homogeneous cosmological degrees of freedom

$$S_{\text{eff}} = \int d\tau \left\{ \begin{array}{c} -\frac{1}{2e}\left(\partial_\tau(a\phi)\right)^2 + \frac{1}{2e}\left(\partial_\tau(as)\right)^2 + \frac{\kappa^2}{12e}\left(\phi^2 - s^2\right)a^2\left(\dot{\alpha}_1^2 + \dot{\alpha}_2^2\right) \\ -e\left[a^4\phi^4 f\left(\frac{s}{\phi}\right) + \rho_r - \frac{1}{2}\left(\phi^2 - s^2\right)a^2 v(\alpha_1, \alpha_2)\right], \end{array} \right\} \tag{11}$$

where ρ_r is the radiation density when the scale factor $a = 1$. The effective action is invariant under time dependent Weyl transformations

$$a(\tau) \to \Omega^{-1}(\tau)\, a(\tau), \ \left(\phi(\tau), s(\tau)\right) \to \Omega(\tau)\left(\phi(\tau), s(\tau)\right) \tag{12}$$

while $\alpha_{1,2}$ and e are Weyl invariant. Here $v(\alpha_1, \alpha_2)$ is the anisotropy potential which emerges from the curvature term $\left(\phi^2 - s^2\right)R(g)$

$$v(\alpha_1, \alpha_2) = \frac{K}{1 - 4\ \text{sign}(K)} \left[\begin{array}{c} e^{-4\sqrt{2/3}\kappa\alpha_1} + 4e^{2\sqrt{2/3}\kappa\alpha_1}\sinh^2\left(\sqrt{2}\kappa\alpha_2\right) \\ -4\ \text{sign}(K)\ e^{-\sqrt{2/3}\kappa\alpha_1}\cosh\left(\sqrt{2}\kappa\alpha_2\right) \end{array} \right]. \tag{13}$$

In the isotropic limit the anisotropy potential reduces to a constant $\lim_{\alpha_{1,2}\to 0} v(\alpha_1,\alpha_2) = K$. For the Kasner metric the potential energy term is absent even if anisotropy is present since $K = 0$.

For the cosmological solutions discussed in this paper we will concentrate on the isotropic case $\alpha_{1,2} \to 0$, and therefore $v(\alpha_1,\alpha_2) \to K$. The generalization of our discussion to homogeneous and anisotropic universes is given in [17] and [18].

In this action $e(\tau)$ is related to the lapse function which is a part of the metric $g_{\mu\nu}(x)$. Its presence insures τ-reparameterization symmetry. The equation of motion with respect to e imposes a constraint on the degrees of freedom. This constraint is equivalent to the $G_{00} = T_{00}$ Einstein equation. One may choose a gauge for τ, such that $e(\tau) = 1$, in which case the action simplifies.

In the Einstein gauge of Eq.(6) the cosmological action is

$$S_{\text{eff}}^{E} = \int d\tau \left\{ \begin{array}{c} \frac{1}{e}\left[-\frac{6}{2\kappa^2}\dot{a}_E^2 + \frac{1}{2}a_E^2\dot{\sigma}^2 + \frac{1}{2}a_E^2\dot{\alpha}_1^2 + \frac{1}{2}a_E^2\dot{\alpha}_2^2\right] \\ -e\left[a_E^4 V(\sigma) + \rho_r - \frac{6}{2\kappa^2}a_E^2 v(\alpha_1,\alpha_2)\right] \end{array} \right\}. \tag{14}$$

In this action note that the $a_E(\tau)$ degree of freedom has the wrong sign kinetic energy term, and therefore it is potentially a ghost. However, the Hamiltonian derived from this action in the $e(\tau) = 1$ gauge is required to vanish as a result of the constraint, and this is just sufficient to compensate for the ghost. This constraint equation, which is called the zero energy condition, is the same as the first Friedmann equation.

The γ-gauge is defined by fixing

$$a_\gamma(\tau) = 1 \tag{15}$$

for all τ. In the γ-gauge, the cosmological action is

$$S_{\text{eff}}^{\gamma} = \int d\tau \left\{ \begin{array}{c} \frac{1}{e}\left[-\frac{1}{2}\dot{\phi}_\gamma^2 + \frac{1}{2}\dot{s}_\gamma^2 + \frac{\kappa^2}{12}\left(\phi_\gamma^2 - s_\gamma^2\right)\left(\dot{\alpha}_1^2 + \dot{\alpha}_2^2\right)\right] \\ -e\left[\phi_\gamma^4 f(s_\gamma/\phi_\gamma) + \rho_r - \frac{1}{2}\left(\phi_\gamma^2 - s_\gamma^2\right)v(\alpha_1,\alpha_2)\right] \end{array} \right\}. \tag{16}$$

When $V(\sigma)$ is given as in Eq. (1), then $\phi_\gamma^4 f(s_\gamma/\phi_\gamma) = b\phi_\gamma^4 + cs_\gamma^4$ is purely quartic. In this action the ϕ_γ degree of freedom has the wrong sign kinetic energy term. However, as in the case of a_E in the previous paragraph, due to the τ-reparameterization symmetry, and the corresponding zero energy constraint that follows from the equation for e, this potential ghost is eliminated.

We can relate the E-gauge and γ-gauge degrees of freedom to each other by a gauge transformation. More easily, we identify the gauge invariants χ and s/ϕ in both gauges, and from them we extract

$$a_E^2 = \frac{\kappa^2}{6} \left|\phi_\gamma^2 - s_\gamma^2\right|, \; \sigma = \frac{\sqrt{6}}{2\kappa} \ln \left(\left| \frac{\phi_\gamma + s_\gamma}{\phi_\gamma - s_\gamma} \right| \right). \tag{17}$$

From this, we see that, what appeared as a cosmological singularity in the E-gauge at $a_E^2(\tau_B) = 0$ does not show up at all as a geometrical singularity in the γ-gauge since $R_{\mu\nu\lambda\sigma}(\eta) = 0$. Of course, the big bang of the E-gauge must reflect itself again as the gauge invariant $\chi(\tau_B) = 0$, which becomes $(\phi_\gamma^2 - s_\gamma^2)(\tau_B) \to 0$, however this is not a singularity of the equations within the γ-gauge.

The absence of a geometrical singularity in the γ-gauge, and the simplicity of the equations of motions for ϕ_γ, s_γ is the key for being able to solve all the cosmological equations and finding the complete set of solutions analytically. This is also what permits us to understand geodesic completeness. The geodesically complete geometry includes space-time regions of *antigravity*. In the antigravity regions the gravitational parameter $\frac{1}{12}(\phi^2 - s^2)$ that appears in the general action becomes negative. The switching of the sign in generic solutions of the theory occurs precisely at $\chi(\tau_B) = 0$, which appears as the cosmological singularity in the E-gauge, but this is a completely smooth point for the geometry in the γ-gauge, as well as all other gauges, except the E-gauge.

Supergravity gauge (c-gauge): In the c-gauge [20], we fix $\phi_c = \phi_0$ where ϕ_0 is a constant for all x^μ. Then in (3) or (11) there is only one scalar $s_c(x)$ while the curvature term takes the form $\frac{1}{12}(\phi_0^2 - s_c^2(x)) R(g_c(x))$. We see that the ϕ_0^2 term plays the role of the Hilbert-Einstein term while the overall structure $\frac{1}{12}(\phi_0^2 - s_c^2) R(g_c)$ is similar to that found in supergravity, including the Kähler potential. In fact, this model can be regarded as a toy model for the scalar sector of a full supergravity model. Then the term $(-s_c^2 R(g_c))$ allows us to identify $s_c^2(x)$ as the analog of the Kähler potential in supergravity. The gauge invariant becomes $\chi \equiv \frac{\kappa^2}{6}(-g_c)^{\frac{1}{4}}(\phi_0^2 - s_c^2(x))$, and for a cosmological solution it takes the form

$$\chi = \frac{\kappa^2}{6}(\phi_0^2 - s_c^2(\tau)) a_c^2(\tau). \tag{18}$$

Since we have all the solutions, we can verify that the cosmological singularity $\chi(\tau_B) = 0$, which in the Einstein frame is at $a_E(\tau_B) = 0$, occurs when $s_c^2(\tau_B) = \phi_0^2$, rather than $a_c^2(\tau_B) = 0$. Hence the metric $g_c^{\mu\nu}$ in this gauge is not singular at the Big Bang. This is because the quantity $s_c/\phi_0 = s_\gamma/\phi_\gamma = s_E/\phi_E$ is gauge invariant and takes the value $(s/\phi)(\tau_B) \to 1$ at the singularity in any gauge. (The reason that the E-gauge $\frac{1}{12}(\phi_E^2(x) - s_E^2(x)) = (2\kappa^2)^{-1}$ can remain finite even at the singularity $\chi(\tau_B)=0$, is because in the expression $(\phi_E^2-s_E^2)(\tau_B)=\phi_E^2(\tau_B)(1-s_E^2/\phi_E^2)(\tau_B)$, when the second factor vanishes, the factor $\phi_E^2(\tau_B)$ blows up so that $(\phi_E^2-s_E^2)$ remains unchanged at all x^μ, including at the singularity at time τ_B.) This shows that, similar to $\frac{1}{12}(\phi_0^2-s_c^2)R(g_c)$, the effective gravitational constant in the curvature term in the action of a supergravity theory is typically expected to switch sign at the big crunch or big bang. So the phenomena we discuss here, including antigravity regimes related to geodesic completeness, are expected generically in typical supergravity theories.

String gauge (s-gauge): We also discuss the string gauge (s-gauge) to connect to the typical structures in string theory. The string frame in d dimensions is defined by the following form of Lagrangian

$$L_{\text{string gauge}}=\frac{1}{2\kappa^2}e^{-\sqrt{\frac{d-2}{2}}\Phi}\left(R(g_s)+\frac{d-2}{2}g_s^{\mu\nu}\partial_\mu\Phi\partial_\nu\Phi-V_s(\Phi)\right), \tag{19}$$

Note the wrong sign and unusual normalization of the kinetic term for the "dilaton" Φ . When the transformation from the string-frame to the E-frame is performed by the substitution

$$(g_s)_{\mu\nu}=e^{\sqrt{\frac{2}{d-2}}\Phi}(g_E)_{\mu\nu},\ \Phi=\sqrt{2\kappa^2}\sigma, \tag{20}$$

then the right sign and normalization of the Einstein-frame σ field emerges

$$L_{\text{Einstein gauge}}=\left(\frac{1}{2\kappa^2}R(g_E)-\frac{1}{2}g_E^{\mu\nu}\partial_\mu\sigma\partial_\nu\sigma-V(\sigma)\right). \tag{21}$$

The string gauge in Eq.(19), for $d=4$, is obtained from our Weyl invariant action (3) by choosing the following gauge in which ϕ_s,s_s are expressed in terms of a single scalar Φ (this is analogous to ϕ_E,s_E given in Eq.(6))

$$\phi_s(x)=\frac{\sqrt{6}}{\kappa}e^{-\frac{1}{2}\Phi(x)}\cosh\left(\sqrt{\frac{1}{12}}\Phi(x)\right),$$
$$s_s(x)=\frac{\sqrt{6}}{\kappa}e^{-\frac{1}{2}\Phi(x)}\sinh\left(\sqrt{\frac{1}{12}}\Phi(x)\right),$$

while the metric $g_s^{\mu\nu}$ is labelled with the letter s to distinguish it from the metric in another Weyl gauge. This shows how the dilaton field Φ of the non-Weyl invariant string theory can be related to the fields ϕ,s in the Weyl invariant theory.

Then the effective cosmological action in the string gauge takes the form of Eq.(11) where the gauge fixed form for (ϕ_s,s_s) is inserted. The remaining degrees of freedom in the string gauge are then (a_s, σ) ,where σ is the same field as the one in the Einstein gauge except for the overall normalization in Eq.(20), while a_s is related to a_E simply by the transformation in Eq.(20) for $d = 4$

$$a_s^2 = e^{\sqrt{2\kappa^2}\sigma} a_E^2, \;\; \Phi = \sqrt{2\kappa^2}\sigma. \tag{22}$$

Therefore, by using the relation between the E-gauge and the γ-gauge in (17), we can relate the s-gauge degrees of freedom, a_s, Φ, to the γ-gauge degrees of freedom as follows

$$\begin{aligned} a_s^2 &= \frac{\kappa^2}{6} \left| \frac{\phi_\gamma + s_\gamma}{\phi_\gamma - s_\gamma} \right|^{\sqrt{3}} \left(\phi_\gamma^2 - s_\gamma^2 \right) \\ \Phi &= \sqrt{3} \ln \left| \frac{\phi_\gamma + s_\gamma}{\phi_\gamma - s_\gamma} \right| \end{aligned} \tag{23}$$

The expressions given above are consistent with the gauge invariants $\chi, (s/\phi), a\phi, as,$ as expressed in the s, γ, E, c-gauges, such as $a_s\phi_s = a_E\phi_E = a_c\phi_c = a_\gamma\phi_\gamma$, etc.

In solving the cosmological equations various gauge choices turn out to be useful. In particular, for the cases we have solved, the γ-gauge turned out to be the most useful. By using the relations between gauges displayed above, the solutions for $\phi(\tau), s_\gamma(\tau)$ imply the solutions of the degrees of freedom in the other gauge choices.

III. SOLVING THE EQUATIONS WITH RADIATION AND CURVATURE

The crucial step introduced in [14], as suggested by 2T-physics, is to take advantage of the gauge symmetry of the conformally invariant action (3). The Einstein equations derived from the action (3), taken with only time dependent isotropic fields, yields gauge covariant cosmological equations for three fields $a(\tau), \phi(\tau), s(\tau)$ in any gauge. If one chooses the Einstein gauge given in Eq. (6) then the corresponding gauge fixed fields $a_E(\tau), \sigma(\tau)$ satisfy the Friedmann equations including radiation ρ_r, as given below in Eqs.(25-27). Instead, if one chooses the γ-gauge defined by $a_\gamma(x) = 1$, the remaining fields $\phi_\gamma(\tau), s_\gamma(\tau)$ turn out to satisfy the decoupled equations (28-30) that can be solved exactly. Then, by performing a gauge transformation that relates the two gauge fixed configurations we obtain the full set of solutions of the Friedmann equations.

The field re-definition from σ, a_E to ϕ_γ, s_γ, is derived from the gauge transformation that connects the E and γ gauges [14] and is given in Eq. (17). Note that generically $\chi(x^\mu)$ can be positive or negative. But the metric in the Einstein gauge, in either the gravity or antigravity patches, has always the correct signature metric, hence, the absolute value in the relation for a_E^2 in Eq. (17). The inverse of the transformation (17) involves four quadrants in the (ϕ_γ, s_γ) space depicted in Fig. 1, and is given by

$$\phi_\gamma = \pm \begin{cases} \frac{\sqrt{6}}{\kappa}\sqrt{|\chi|}\cosh\left(\frac{\kappa\sigma}{\sqrt{6}}\right), & \text{if } \chi > 0 \\ \frac{\sqrt{6}}{\kappa}\sqrt{|\chi|}\sinh\left(\frac{\kappa\sigma}{\sqrt{6}}\right), & \text{if } \chi < 0 \end{cases}, \quad s_\gamma = \pm \begin{cases} \frac{\sqrt{6}}{\kappa}\sqrt{|\chi|}\sinh\left(\frac{\kappa\sigma}{\sqrt{6}}\right), & \text{if } \chi > 0 \\ \frac{\sqrt{6}}{\kappa}\sqrt{|\chi|}\cosh\left(\frac{\kappa\sigma}{\sqrt{6}}\right), & \text{if } \chi < 0 \end{cases}. \tag{24}$$

As indicated in Fig. 1, in the gravity sector (left/right quadrants) $\chi(x^\mu)$ is positive, while it is negative in the antigravity sector (top/bottom quadrants).

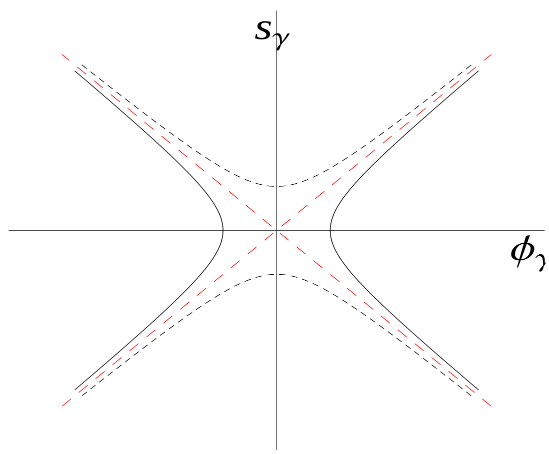

FIG. 1: The gravity regime ($\phi_\gamma^2 > s_\gamma^2$) is in left and right quadrants and the antigravity regime ($\phi_\gamma^2 < s_\gamma^2$) is in top and bottom quadrants.

The transformations (17) and (24) can be used by starting directly from the original action (2) without ever mentioning the Weyl symmetry or the Einstein gauge. Furthermore, it can be used for any spacetime dependence of the fields $\sigma(x), a_E(x)$, $\phi_\gamma(x), s_\gamma(x)$ to rewrite all equations in terms of $\phi_\gamma(x), s_\gamma(x)$ rather than $\sigma(x), a_E(x)$. If used in that sense then it can be considered to be an analog of what the Kruskal-Szekeres coordinates are to the Schwarzchild coordinates in the description of the black hole spacetime. Namely, they demonstrate that the spacetime regions across the horizon are smoothly geodesically connected. The analog here is that the field space regions $(\phi_\gamma^2 - s_\gamma^2) > 0$ and $(\phi_\gamma^2 - s_\gamma^2) <$ 0 are naturally connected at $\phi_\gamma^2 = s_\gamma^2$; hence, the patches of spacetime x^μ in which each inequality is satisfied are connected geodesically, as seen in our purely time dependent solutions. Note that, in the $\phi_\gamma(\tau), s_\gamma(\tau)$ form, the Friedmann equations (28-30) do not display any singularities. Further thought suggests that the connection $\phi_\gamma^2(x^\mu) = s_\gamma^2(x)$ (which corresponds to the dashed 45 degree lines in field space in Fig. 1) can occur only at spacetimes x^μ at which the curvature in the Einstein frame diverges $R(g_E(x)) = \infty$.

Inserting the above field redefinition into the standard Friedmann equations and equation of motion for σ in the isotropic limit (derived from the action in (2) or (14)),

$$\frac{\dot{a}_E^2}{a_E^4} = \frac{\kappa^2}{3}\left[\frac{\dot{\sigma}^2}{2a_E^2} + V(\sigma) + \frac{\rho_r}{a_E^4}\right] - \frac{K}{a_E^2} \tag{25}$$

$$\frac{\ddot{a}_E}{a_E^3} - \frac{\dot{a}_E^2}{a_E^4} = -\frac{\kappa^2}{3}\left[\frac{\dot{\sigma}^2}{a_E^2} - V(\sigma) + \frac{\rho_r}{a_E^4}\right], \tag{26}$$

$$\frac{\ddot{\sigma}}{a_E^2} + 2\frac{\dot{a}_E\dot{\sigma}}{a_E^3} + V'(\sigma) = 0, \tag{27}$$

where dot denotes derivative with respect to the conformal time τ, we obtain

$$0 = \ddot{\phi}_\gamma - 4b\phi_\gamma^3 + K\phi_\gamma, \tag{28}$$

$$0 = \ddot{s}_\gamma + 4cs_\gamma^3 + Ks_\gamma, \tag{29}$$

$$0 = -\left(\frac{1}{2}\dot{\phi}_\gamma^2 - b\phi_\gamma^4 + \frac{1}{2}K\phi_\gamma^2\right) + \left(\frac{1}{2}\dot{s}_\gamma^2 + cs_\gamma^4 + \frac{1}{2}Ks_\gamma^2\right) + \rho_r. \tag{30}$$

These are precisely the equations of motion derived from the isotropic limit of the action (3) in the $a_\gamma = 1$ gauge [14]. The fields ϕ_γ, s_γ are decoupled except for the zero energy condition in Eq. (30). These equations are valid not only when $\chi > 0$ but also when $\chi < 0$, hence, they provide a smooth continuation from the gravity sector to the antigravity sector. The question is whether this continuation is required by the dynamics as part of the evolution of the universe in a geodesically complete geometry. We demonstrate that the generic geodesically complete solutions do require this continuation.

Integrating the first two equations, and using the energy constraint, leads to the following decoupled first order differential equations

$$\frac{1}{2}\dot{\phi}_\gamma^2 - b\phi_\gamma^4 + \frac{K}{2}\phi_\gamma^2 = E_\phi, \quad \frac{1}{2}\dot{s}_\gamma^2 + cs_\gamma^4 + \frac{K}{2}s_\gamma^2 = E_s, \tag{31}$$

with a relation between the two integration constants (E_ϕ, E_s) that reduces the unknowns to the single energy parameter E

$$E_s \equiv E, \; E_\phi = E + \rho_r. \tag{32}$$

Equations (31) are analogous to the equations satisfied by two non-relativistic particles with "position" coordinates, ϕ_γ and s_γ, moving independently from each other as controlled by the potentials $V(\phi_\gamma) = -b\phi_\gamma^4 + \frac{K}{2}\phi_\gamma^2$ and $V(s_\gamma) = cs_\gamma^4 + \frac{K}{2}s_\gamma^2$, at energy levels $E_\phi = E + \rho_r$ and $E_s = E$ respectively. So, the nature of the solution and the corresponding physics is easily obtained through this analogy. It is sufficient to draw a picture of the potentials $V(\phi_\gamma), V(s_\gamma)$ and indicate the energy levels $E_\phi = E + \rho_r$ and $E_s = E$ on these pictures, and then let each particle begin its motion at some arbitrary points. The reader is invited to examine the figures in the Appendix to follow our arguments below.

We can choose to begin the motion at τ_0 with initial values $\phi_\gamma(\tau_0), s(\tau_0)$ that insure the gauge invariant factor $(1 - s^2/\phi^2)$ is positive in all gauges at the initial time τ_0 . Due to the time translation symmetry one of these initial values may be fixed once and for all without losing generality. For example, we may begin the motion somewhere on the horizontal line in Fig. 1 which is in the gravity sector in any gauge

$$\left(1 - s^2(\tau_0)/\phi^2(\tau_0)\right) = \left(1 - s_\gamma^2(\tau_0)/\phi_\gamma^2(\tau_0)\right) = 1 > 0. \tag{33}$$

This motion begins in the right or left quadrants and can be described initially by choosing the Einstein gauge (6). The ensuing motion gives the time dependence of the generic solution $\phi_\gamma(\tau)$ and $s_\gamma(\tau)$. The solution is controlled by 6 parameters, namely the four parameters that define the model (b, c, K, ρ_r), one initial value energy parameter E and one initial value $\phi_\gamma(\tau_0)$. We need to analyze various regions of the 6-parameter space because the motion can be qualitatively different in different ranges of the parameters. This is easily seen by staring at the pictures of the potentials in the Appendix (see [15] for the discussion).

The generic motion is oscillatory with each particle moving independently with independent oscillation periods. Each particle may pass through zero at various times independently from each other. Hence $\left(\phi_\gamma^2(\tau) - s_\gamma^2(\tau)\right)$ keeps changing sign in the γ-gauge for the generic solution. This shows that generically the *gauge invariant factor* $\left(1 - s_\gamma^2(\tau)/\phi_\gamma^2(\tau)\right)$, which is the same in every gauge $\left(1 - s_\gamma^2(\tau)/\phi_\gamma^2(\tau)\right) = (1 - s^2(\tau)/\phi^2(\tau))$, changes sign periodically at times $\tau = \tau_n$ in *every gauge*, where τ_n is defined by the zeros of the gauge invariant factor computed in the γ-gauge $\left(1 - s_\gamma^2(\tau_n)/\phi_\gamma^2(\tau_n)\right) = 0$. At precisely these times the scale factor in the Einstein gauge vanishes as seen from Eq. (17), $a_E^2(\tau_n) = \frac{\kappa^2}{6}\left(\phi_\gamma^2(\tau_n) - s_\gamma^2(\tau_n)\right) = 0$, and hence, this is when there is a big bang or a big crunch. In the Einstein gauge the generic motion must be terminated artificially at these instants of time since a_E^2 is positive by definition. However, in the ϕ_γ, s_γ space the motion continues smoothly to the antigravity regime where $\phi^2(\tau) < s^2(\tau)$, which shows that the Einstein frame is geodesically incomplete for the generic motion. There exists a special subset of solutions that is geodesically complete in the Einstein frame without wandering into the antigravity sector, but for now let us continue with the generic motion.

We have seen that even though the motion began in the gravity sector in Fig. 1 the particle reaches some point on the "light cone" in (ϕ, s) space where $\phi^2(\tau_1) = s^2(\tau_1)$ at $\tau = \tau_1$ in any gauge; it then moves smoothly into the antigravity region where $\phi^2(\tau) < s^2(\tau)$ for some period of time $\tau_1 < \tau < \tau_2$. It then turns around and passes through some other point on the lightcone at $\phi^2(\tau_2) = s^2(\tau_2)$ at $\tau = \tau_2$, thus reaching the gravity region again. The generic motion continues periodically in this way, oscillating back and forth between the gravity and the antigravity regions. This generic motion is represented by a curve in the (ϕ_γ, s_γ) plane. Since we have the analytic solutions, we can construct the curve explicitly as a parametric plot $\phi_\gamma(\tau), s_\gamma(\tau)$ as shown in Fig. 2. The precise curve of the parametric plot is determined by the values of the 6 parameters $(b, c, K, \rho_r, E, \phi(\tau_0))$. Generically the curve winds around the (ϕ_γ, s_γ) plane since $\phi_\gamma(\tau), s_\gamma(\tau)$ are each periodic, although their periods are generically incommensurate. The curve becomes a closed curve if the ratio of the periods is a rational number. This indicates that the generic solution has repeated big bangs and crunches and can be cyclic when the periods are commensurate. Within each cycle there is *a period of antigravity sandwiched between every crunch and the following big bang.*

The mathematical expressions of the solutions are given in the Appendix. The methods we used here follow those of [14, 15]. The solutions are parametrized in terms of Jacobi elliptic functions $sn(z|m)$, $cn(z|m)$, $dn(z|m)$ [29] in combinations chosen appropriately in all the relevant regions of the parameter space. For example, in a given region of parameter space the solution looks like

$$\phi_\gamma(\tau) = A\frac{sn(\frac{\tau+\tau_0}{T}|m)}{dn(\frac{\tau+\tau_0}{T}|m)}, \tag{34}$$

with a similar expression for $s_\gamma(\tau)$, where the factors A, T, m are determined in terms of the 6 parameters $(b, c, K, \rho_r, E, \phi(\tau_0))$. The interested reader will find these expressions in our recent paper [15] for the case of $\rho_r = 0$. The only modification to generalize to $\rho_r \neq 0$ is that previously we had used $E_\phi = E_s = E$, while presently we have $E_s = E$ and $E_\phi = E + \rho_r$. Since $E_\phi \geq E_s$ due to $\rho_r \geq 0$, there are more cases to investigate depending on the regions of the parameter space.

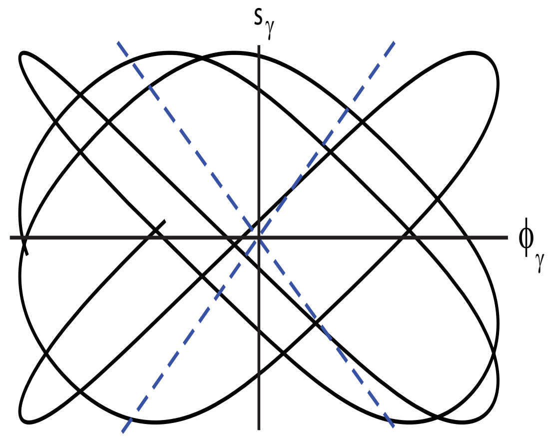

FIG. 2: The generic isotropic solution crosses back and forth through the gravity (left and right quadrants) and antigravity (top and bottom) quadrants.

IV. GEODESICALLY COMPLETE BOUNCES WITHOUT ANTIGRAVITY

Are there solutions that avoid the antigravity period in the cycle? Yes, there is a subset of the parameter space for which the universe completely avoids antigravity. Although this behavior is not generic, such solutions can be characterized as the only ones that are geodesically complete in only the gravity regime of the Einstein frame, which means they are fully described by the action (2) with the additional condition of geodesic completeness. This special subset is obtained by demanding that $|\phi_\gamma(\tau)| \geq |s_\gamma(\tau)|$ at all times. So for the solutions of $\phi_\gamma(\tau)$ that oscillate between positive and negative values, at the points in time when $|\phi_\gamma(\tau)|$ vanishes $|s_\gamma(\tau)|$ must also vanish. This is possible only if the period of ϕ is an integer multiple of the period of s. Since there is a time translation symmetry in the differential equations, without losing generality we can choose that the first instance they both vanish is at $\tau = 0$. Hence, for $\phi_\gamma(\tau), s_\gamma(\tau)$ we must require $\phi_\gamma(0) = s_\gamma(0) = 0$ which synchronizes their initial values to be both zero. This point in time is the big bang since we compute from Eq. (17) that at this time the scale factor vanishes $a_E(0) = 0$. There are regions of parameter space that yield such solutions, but as compared to the full 6-parameter space it may be considered a set of measure zero. In the case of no radiation, $\rho_r = 0$, this geodesically complete subset of solutions is given analytically in [15].

A special example of such a solution is given in the parametric plot in Fig. 3 borrowed from [15]. This is a solution in a region of the parameter space where there is no radiation $\rho_r = 0$;

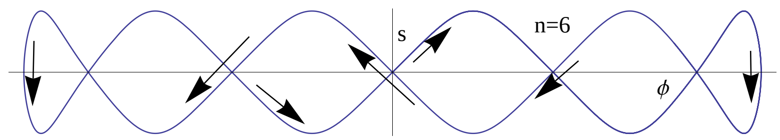

FIG. 3: Non-generic, zero-size bounce cyclic solution that never crosses into the antigravity region. This figure is for $b<0$ and $c>0$. If $b,c>0$ the figure extends to ∞ in the ϕ direction (see [15]).

no curvature $K=0$; special initial conditions $\phi_\gamma(0)=s_\gamma(0)=0$; and a quantized relation $b=-c/n^4$ for integer n. This quantization arises from asking the relative quantization of the periods for ϕ,s. Besides these restrictions the parameters are free to be in the regions $c>0$, $E>0$ and $n\geq 2$.

In Fig. 3, with $n=6$, the fields ϕ_γ, s_γ start out initially both vanishing $\phi_\gamma(0)=s_\gamma(0)=0$ at the big bang (the arrow at the origin of the figure); then while $\phi_\gamma(\tau)$ keeps growing, the field $s_\gamma(\tau)$ oscillates several times until $\phi_\gamma(\tau)$ reaches its maximum and turns around; then $\phi_\gamma(\tau)$ decreases to zero while $s_\gamma(\tau)$ oscillates several times and vanishes at the same time as ϕ_γ. This point in time represents a big crunch. Then the motion continues smoothly to negative values of ϕ_γ and repeats the same behavior of big bang then turnaround and big crunch. The full cycle is repeated again and again periodically which is described by Fig. 5 in the Appendix. Note the 5 nodes in this figure are determined by the choice of the integer $n=6$.

When $\rho_r>0$, the quantization requirement for the periods puts a less severe restriction on the parameters $(b,c,K,\rho_r,E,\phi(\tau_0))$. Although the synchronization of initial conditions $\phi(0)=s(0)=0$ and the relative quantization of the periods are still necessary, these conditions no longer require that b/c is quantized by itself because the additional parameter ρ_r also enters in the quantization of the periods. Instead, the parameters (b,c,K,ρ_r,E) collectively are subject to one quantization condition; *e.g.;* the integration parameter E may be quantized in terms of the other four parameters plus an integer. An example of such a solution with radiation (but with $K=0$ for illustration) is given in the first line of Table I, by the parameters that satisfy $\frac{b(E+\rho_r)}{cE}=\frac{-1}{n^4}$, with $n=$ integer. This is solved by a quantized integration parameter $E_n=-\frac{b\rho_r n^4}{bn^4+c}$. On the other hand when ρ_r vanishes we have, $\frac{b(E+0)}{cE}=\frac{-1}{n^4}$, where the parameter E drops out and there is a solution like the one in Fig. 3, only if the parameters of the model are quantized $b=-c/n^4$. The inclusion of radiation changes the parametric plot above in a simple way: the trajectory extends further out in the ϕ_γ direction as ρ_r increases due to the higher energy in the ϕ_γ field.

We list below all the cases of parameter subspaces that permit purely gravity (i.e. no antigravity regime) geodesically complete solutions and point out the corresponding figures and formulas shown in the Appendix. All of these describe a universe that always remains in the gravity regime of the Einstein frame, and either: (i) bounces at zero size for $K = 0$; (ii) bounces at zero size for $K \neq 0$; or (iii) bounces at finite size for $K > 0$. These are found by setting

$$\phi(0) = s(0) = 0, \tag{35}$$

(which implies $\delta = 0$) and then replacing $E_\phi = E + \rho_r$ and $E_s = E$, instead of $E_\phi = E_s = E$, in the quantization of the periods. These necessary conditions cannot be satisfied for all the solutions given in the figures in the Appendix; the cases that are compatible with these conditions are indicated on the right side of Tables I,IIa,IIb,III.

- If $K = 0$, there are two regimes of parameter space in which there can be a singular bounce without violating the null energy condition:

	b	c	E	ρ_r	Table I: conditions when $K = 0$	FIG #
1.	< 0	> 0	> 0	≥ 0	$\frac{b(E+\rho_r)}{cE} = \frac{-1}{n^4}, \begin{cases} n = 1,2,3\ldots \text{if } \rho_r > 0 \\ n = 2,3,4\ldots \text{ if } \rho_r = 0 \end{cases}$	Fig.5
2.	> 0	> 0	> 0	≥ 0	$\frac{b}{4c}\frac{E+\rho_r}{E} = \frac{1}{n^4},\ n = 1,2,3\ldots$	Fig.6

- If $K > 0$, there exist two categories of cyclic solutions, the ones that bounce at zero size without violating the null energy condition, and the ones that bounce at finite size.

The conditions on the parameters for *bouncing at finite size* are

	b	c	$E+\rho_r$	ρ_r	Table IIa: conditions when $K>0$	FIG #
1.	>0	>0	$\geq 0, \leq \frac{K^2}{16b}$	$< \frac{K^2}{16b}$	$\lvert\phi(\tau_0)\rvert \geq \sqrt{\frac{K}{4b}}$	Fig.12
2.	>0	<0	$>0, \leq \frac{K^2}{16b}$	$< \frac{K^2}{16b}$	$\lvert\phi(\tau_0)\rvert \geq \sqrt{\frac{K}{4b}}, \lvert s(\tau_0)\rvert \leq \lvert\phi(\tau_0)\rvert$	Fig.18

The conditions on the parameters for *bouncing at zero size* are given below. In these expressions $\mathcal{K}(m) \equiv EllipticK(m)$ is a well known special function that corresponds to the quarter period of the Jacobi elliptic functions, such as $sn(z|m)$, with label m [29].

	b	c	$E+\rho_r$	ρ_r	Table IIb: conditions when $K>0$	FIG #
1.	≤ 0	>0	>0	≥ 0	$\frac{\left(1+\frac{16c}{K^2}E\right)^{1/4}\times\mathcal{K}\left(\frac{1}{2}-\frac{1}{2}\left(1-\frac{16b}{K^2}(E+\rho_r)\right)^{-1/2}\right)}{\left(1-\frac{16b}{K^2}(E+\rho_r)\right)^{1/4}\times\mathcal{K}\left(\frac{1}{2}-\frac{1}{2}\left(1+\frac{16c}{K^2}E\right)^{-1/2}\right)} = n$ $\begin{cases} n=1,2,3\ldots \text{if } \rho_r>0 \\ n=2,3,4\ldots \text{ if } \rho_r=0 \end{cases}, E>0$	Fig.10
2.	>0	≥ 0	$> \frac{K^2}{16b}$	≥ 0	$\frac{\sqrt{2}\left(1+\frac{16c}{K^2}E\right)^{1/4}\times\mathcal{K}\left(\frac{1}{2}+\frac{1}{2}\left(\frac{16b}{K^2}(E+\rho_r)\right)^{-1/2}\right)}{\left(\frac{16b}{K^2}(E+\rho_r)\right)^{1/4}\times\mathcal{K}\left(\frac{1}{2}-\frac{1}{2}\left(1+\frac{16c}{K^2}E\right)^{-1/2}\right)} = n$ $n=1,2,3\ldots$	Fig.13
3.	>0	≥ 0	≥ 0	≥ 0	$\frac{\left(1+\frac{16Ec}{K^2}\right)^{1/4}\times\mathcal{K}\left(\left(\frac{1}{2}+\frac{1}{2}\sqrt{1-\frac{16b}{K^2}(E+\rho_r)}\right)^{-1}-1\right)}{\left(\frac{1}{2}+\frac{1}{2}\sqrt{1-\frac{16b}{K^2}(E+\rho_r)}\right)^{1/2}\times\mathcal{K}\left(\frac{1}{2}-\frac{1}{2}\left(1+\frac{16Ec}{K^2}\right)^{-1/2}\right)} = n$ $n=1,2,3\ldots, E+\rho_r \leq \frac{K^2}{16b}, \lvert\phi_\gamma(\tau_0)\rvert < \sqrt{\frac{K}{4b}}$	Fig.11
4.	>0	<0	$> \frac{K^2}{16b}$	≥ 0	$\frac{\sqrt{2}\left(\frac{1}{2}+\frac{1}{2}\sqrt{1+\frac{16cE}{K^2}}\right)^{1/2}\times\mathcal{K}\left(\frac{1}{2}+\frac{1}{2}\sqrt{\frac{16b}{K^2}(E+\rho_r)}\right)}{\left(\frac{16b}{K^2}(E+\rho_r)\right)^{1/4}\times\mathcal{K}\left(\left(\frac{1}{2}+\frac{1}{2}\sqrt{1+\frac{16cE}{K^2}}\right)^{-1}-1\right)} = n$ $n=1,2,3\ldots, \frac{K^2}{16(-c)} > E > 0,\ \lvert s_\gamma(\tau_0)\rvert < \sqrt{\frac{K}{4(-c)}}$	Fig.17
5.	>0	$c<0$	$> \frac{K^2}{16b}$	≥ 0	$\frac{\left(-\frac{16c}{K^2}E\right)^{1/4}*\mathcal{K}\left(\frac{1}{2}+\frac{1}{2}\left(\frac{16b}{K^2}(E+\rho_r)\right)^{-1/2}\right)}{\left(\frac{16b}{K^2}(E+\rho_r)\right)^{1/4}*\mathcal{K}\left(\frac{1}{2}+\left(-\frac{16c}{K^2}E\right)^{-1/2}\right)} = 1;\ \frac{K^2}{16(-c)} < E$	Fig.16

- If $K < 0$, the conditions on the parameters for *bouncing at zero size* are

	b	c	$E+\rho_r$	ρ_r	Table III: condition when $K<0$	FIG #
1.	<0	>0	>0	≥ 0	$\frac{\left(1+\frac{16c}{K^2}E\right)^{1/4}\times\mathcal{K}\left(\frac{1}{2}-\frac{1}{2}\left(1-\frac{16b}{K^2}(E+\rho_r)\right)^{-1/2}\right)}{\left(1-\frac{16b}{K^2}(E+\rho_r)\right)^{1/4}\times\mathcal{K}\left(\left(\frac{1}{2}-\frac{1}{2}\left(1+\frac{16c}{K^2}E\right)^{-1/2}\right)\right)}=n$ $\begin{cases} n=1,2,3\ldots\text{if } \rho_r>0 \\ n=2,3,4\ldots\ \text{if } \rho_r=0 \end{cases}, E>0$	Fig.21
2.	>0	>0	>0	≥ 0	$\frac{\left(1+\frac{16c}{K^2}E\right)^{1/4}\times\mathcal{K}\left(\frac{1}{2}+\frac{1}{2}\left(\frac{16b}{K^2}(E+\rho_r)\right)^{-1/2}\right)}{\sqrt{2}\left(\frac{16b}{K^2}(E+\rho_r)\right)^{1/4}\times\mathcal{K}\left(\frac{1}{2}-\frac{1}{2}\left(1+\frac{16c}{K^2}E\right)^{-1/2}\right)}=n$ $n=1,2,3\ldots, E>0$	Fig.24

- In addition, for any values of b, c, there is the special solution in which $s_\gamma(\tau)=0$ for all τ (sitting at the $s=0$ extremum of $V_s=\frac{1}{2}Ks^2+cs^4$) while $\phi(\tau)$ performs any motion at energy $E_\phi=\rho_r$.

V. GEODESICALLY COMPLETE BOUNCES WITH ANTIGRAVITY

In addition to the solutions described in the previous section, there are ones that are geodesically complete provided an antigravity regime is included (see Fig. 2). In Refs. [17, 18], we show that, when anisotropy is added to the curvature and radiation, there is a strong attractor behavior such that almost all solutions pass through the origin and undergo a period of antigravity (a loop) between each big crunch and big bang. This is illustrated in Fig. 4. As discussed in [17, 18], the zero-size bounce solutions that evolved from crunch to bang in the purely gravity region in the absence of anisotropy (as listed in Tables I,IIb,III) and illustrated in Fig. 3, as well as the other generic solutions in the Appendix illustrated in Fig. 2, are strongly modified near the singularity by the anisotropy, such that the trajectory cannot avoid the antigravity region. Furthermore, given some initial conditions, the global behavior of a trajectory, far away from the singularity, can also be altered even by a small amount of anisotropy [18]. The finite-size bounce solutions could avoid the antigravity region despite anisotropy, but this may occur only in a very narrow region of parameter space.

We are, therefore, faced with trying to understand physical phenomena in the antigravity regime. Since physical intuition for gravity is developed mainly in the Einstein frame, we begin with the Einstein gauge. When (ϕ^2-s^2) is negative, it is again possible to use the

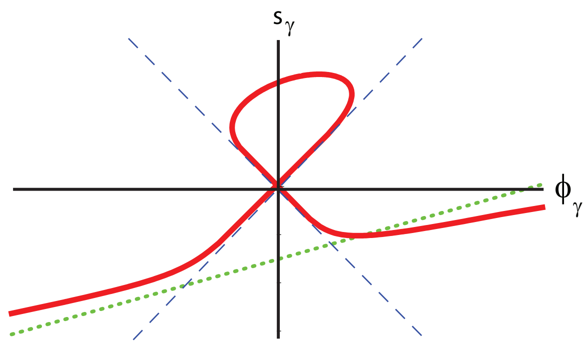

FIG. 4: Comparison of a solution without anisotropy (green dotted path) and with anisotropy added (red thick solid curve). An attractor mechanism caused by the anisotropy distorts the path so that it passes through the origin at the crunch and undergoes a loop in the antigravity region, through the origin again, and then re-emerging in the gravity regime.

Weyl symmetry to choose an Einstein gauge, $\phi_E^2 - s_E^2 = -1/2\kappa^2$, but this is in a new domain of field space, namely in the top and bottom quadrants of the (ϕ, s) space, as shown in Fig. 1. The new ϕ_E, s_E are given by interchanging the sinh and cosh in Eq. (6), namely $\phi_E(x) = \pm\frac{\sqrt{6}}{\kappa}\sinh(\kappa\sigma(x)/\sqrt{6})$, $s_E(x) = \pm\frac{\sqrt{6}}{\kappa}\cosh(\kappa\sigma(x)/\sqrt{6})$, such that $\phi_E^2 - s_E^2 = -1/2\kappa^2$. Then the gauge fixed form of the action (3) looks like the action in Eq. (2), except that the first two terms change sign. The potential $V(\sigma)$ does not change sign, but it is a new function $\bar{V}(\sigma)$, which is related to Eq. (1) by interchanging sinh and cosh. The metric $g_E^{\mu\nu}$ in this gauge has no signature change. Hence, for matter fields, including radiation, the signs of their kinetic terms remain the same in the gravity and antigravity sectors. The gauge-fixed action in the antigravity regime looks as follows

$$S_{antigravity} = \int d^4x\sqrt{-g}\left\{\begin{array}{c} -\frac{1}{2\kappa^2}R(g_E) + \frac{1}{2}g^{\mu\nu}\partial_\mu\sigma\partial_\nu\sigma - \bar{V}(\sigma) \\ +radiation + matter \end{array}\right\}. \qquad (36)$$

Because of the sign change in the first two terms, σ now looks like a ghost while the a_E degree of freedom is no longer a ghost. The zero total energy constraint ($G_{00} = T_{00}$ Einstein equation) compensates for one ghost, as it did in the usual gravity regime, so there are no unitarity. concerns regarding the σ degree of freedom. However, the other fluctuations of the metric, namely the spin-2 gravitons, now have the wrong sign kinetic terms. Note that some of the spin-2 degrees of freedom are in the form of the anisotropy fields; including them does not seem to show any particular instability or other unusual behavior [18].

The discussion of the relativistic harmonic oscillator, as treated in [30], is a good toy model to understand how to correctly quantize the theory while maintaining unitarity when some degrees of freedom have the wrong sign kinetic energy. The basic technique is to interchange the roles of creation-annihilation operators when the kinetic energy has the wrong sign; then the resulting Fock space has only positive norms. As seen in [30] a similar approach also occurs in the construction of unitary representations of non-compact groups by using oscillators. Similarly, in the antigravity regime, the theory should be quantized without negative norm ghosts by interchanging the roles of creation-annihilation operators for gravitons. The price is that the energy of the spin-2 gravitons is unbounded below, so potentially there is an instability. At the linearized level, which defines a perturbative Hilbert space, there is no consequence. But when interactions are included, due to the availability of negative energy states, it may be possible to emit abundantly spin-2 gravitons with negative energy; however this must be accompanied with the emission of positive energy matter to maintain the zero energy constraint. So the theory must react in some interesting ways through the interactions as soon as the antigravity regime is reached.

In the cases where there is anisotropy [17][18], we find that the trajectory of the antigravity depends on the radiation density such that, if ρ_r increases due to the spontaneous production of negative energy gravitons (as noted above), the effect is to decrease the duration of the antigravity period and return the universe more rapidly to the big bang and a period of pure gravity expansion. As noted in [17][31] this is an indication that the dynamics tries to minimize the effects of antigravity, but the details of how this works is currently cloudy.

Of course, quantum gravity effects need to be also included. Therefore, it would be very interesting to study similar circumstances in the framework of string theory. To formulate the antigravity aspects in string theory we could use the field transformations given in Eqs.(17,24), but even better would be the inclusion of the analog of the Weyl symmetry in the framework of string theory.

It is worth mentioning that it seems possible to connect the state of the universe before the crunch to the state of the universe after the crunch by solving our classical equations analytically along a path in the complex τ plane, such that the path completely avoids the antigravity regime, and also stays sufficiently far away from the singularities, so that quantum corrections become negligible. Such an approach is very desirable for the cyclic universe scenario. We will report on this type of solution in a separate paper.

VI. SUMMARY

In this paper we have used analytic solutions of cosmological equations to discuss geodesic completeness through the big bang singularity. In the context of the path integral, our complete set of classical solutions provide a semi-classical approximation to the quantum theory.

The computations presented in this paper mostly ignored anisotropy and used a special potential energy $V(\sigma)$ to obtain *all* the analytic solutions of the Friedmann equations, in a model that includes radiation and spatial curvature. The solutions are characterized by six parameters that include initial values and model parameters. We learned that the generic solution, in which none of the six parameters are restricted, shows that the trajectory of the universe goes smoothly through the crunch/bang singularities while traversing from gravity to antigravity spacetime patches, and doing this repeatedly in a periodic manner. The generic trajectory can cross the "lightcone" in field space, shown in Fig. 1, at any place. The crossing points on the "lightcone" depend on the values of the six parameters. Although our general exact results are obtained in a specific model, the presence of antigravity is likely to occur generically in any model that is geodesically complete. Therefore, the phenomenon of antigravity should be considered seriously in discussing cosmology.

We found that it is possible to avoid antigravity and still have a geodesically complete geometry within a smaller (but still infinite) subset of solutions (Tables I,IIb,III). These are the only geodesically complete solutions contained totally within the traditional Einstein frame. One group of trajectories passes through the center of the "lightcone"repeatedly, resulting in a cyclic universe. These solutions, which do not violate the null energy condition, provide a set of examples that bouncing at zero size is possible classically in cosmological scenarios with or without spatial curvature.

It should be emphasized that our new results transcend the specific simple model above. The phenomena we have found should also be expected generically in supergravity theories coupled to matter whose formulation include a similar factor that multiplies $R(g)$. In supergravity, that factor is related to the Kahler potential, and this factor, combined with the usual Einstein-Hilbert term, is not generally positive definite [32]. In fact, in a gauge that we call the supergravity gauge, or c-gauge, in which $\phi(x)$ is set to a constant ϕ_0 [18, 20], our term $(\phi_0^2 - s^2)R(g)$ reduces precisely to the familiar form in supergravity including a

Kähler-like potential. In the past, it was assumed that the overall factor is positive and investigations of supergravity proceeded only in the positive regime. A discussion of the field space in the positive sector for general $\mathcal{N}$=2 supergravity can be found in [33]. However, our results suggest that generically the overall factor can and will change sign dynamically, in every gauge, and therefore antigravity sectors similar to our discussion in this paper should be expected in typical supergravity theories. This is illustrated with an example in [18].

Until better understood in the context of quantum gravity, or string theory, our results should be considered to be a first pass for the types of new questions they raise and the answers they provide.

Much remains to be understood, including quantum gravity and string theory effects, but it is clear that previously unsuspected phenomena, including antigravity, come into play classically close to the cosmological singularity. The technical tools to study such issues in the context of a full quantum theory of gravity are yet to be developed. This is an important challenge to the theory community, since the results have profound implications for both fundamental physics and our understanding of the origin, evolution and future of the universe.

Acknowledgments

IB and PJS thank the Perimeter Institute for its generous hospitality and support. Research at the Perimeter Institute is support by the Government of Canada and the Province of Ontario through the Ministry of Research and Innovation. This research was also partially supported by the U.S. Department of Energy under grant number DE-FG03-84ER40168 (IB) and under grant number DE-FG02-91ER40671 (PJS).

Appendix A: The Analytic Solutions

The intuitive approach for solving the Friedmann equations in the separable form Eqs.$(28-30)$ was described in Sec. III. In Eqs.(30,32) we showed that a first integral of these second order equations takes the form of the analog problem of a particle in a potential, separately for the "particles" ϕ_γ, s_γ. Namely, $\frac{1}{2}\dot{\phi}_\gamma^2 + V_\phi = E_\phi$, and $\frac{1}{2}\dot{s}_\gamma^2 + V_s = E_s$, with the potentials $V_\phi = -b\phi_\gamma^4 + \frac{K}{2}\phi_\gamma^2$ and $V_s = cs_\gamma^4 + \frac{K}{2}s_\gamma^2$, and also with the energy constraint generally solved by $E_s = E$ and $E_\phi = E + \rho_r$ for any E. In this appendix we list the complete set of analytic solutions to these equations in all possible regions of the six parameter space $(b, c, K, \rho_r, E, \phi(\tau_0))$. In this Appendix, we restrict ourselves to the case $b + c > 0$, which corresponds in the Einstein frame to a potential $V(\sigma)$ in Eq. (1) that is bounded from below. The generalization to unstable potentials is straightforward.

Figs. 5-29 below represent the potentials V_ϕ (solid line) and V_s (dashed line) and the energy levels E_ϕ, E_s; they are drawn in the various regions of parameter space. The ϕ-level $E_\phi = E + \rho_r$ is higher than the s-level $E_s = E$ because the radiation energy density ρ_r is positive. The parameter E is allowed to slide vertically within the physical range permitted for the s-particle's motion in the potential V_s. From the figures alone one can obtain the intuitive solution by invoking the analogy of a particle moving in a potential for either s_γ or ϕ_γ. Next to each figure we give the corresponding analytic solution to Eq.$(28-30)$. We did not include separately some trivial cases such as the case when the fields sit still at the top or bottom of the potential extrema, or in the cases of $b = 0$ or $c = 0$ where Eqs.$(28-30)$ become linear differential equations with simple trigonometric solutions. These cases are recovered in the appropriate limit of the expressions below.

In the analytic expressions below instead of the free parameter $\phi(\tau_0)$ for an arbitrary initial value, we have inserted the arbitrary phase shift parameter δ. Note also that we have used the time translation symmetry of the equations to choose a specific value for the initial value for $s_\gamma(\tau)$ at $\tau = 0$. In this way we give here the generic solutions that describe all possible geodesically complete trajectories of the universe, including those that move between the gravity and antigravity regions.

A subset of solutions stay only in the gravity sector with geodesically complete trajectories. They are obtained by putting constraints on the parameters. These include setting $\delta = 0$ (synchronized initial conditions for ϕ, s) and requiring a quantization of the periods of ϕ relative to the period of s. The corresponding parameter space is given in section (IV).

The reader can verify that the following expressions solve the differential equations and that the plots of $\phi(\tau), s(\tau)$ as functions of τ correspond to the motion intuitively expected for a particle in the corresponding potential at the given energy level. To verify the solution the following properties of the Jacobi elliptic functions $sn(z|m)$, $cn(z|m)$ and $dn(z|m)$ are useful [29]. The derivative of Jacobi elliptic functions are given in terms of expressions somewhat similar to those for trigonometric functions

$$\frac{d}{dz} sn\left(z|m\right) = cn\left(z|m\right) \times dn\left(z|m\right), \tag{A1}$$

$$\frac{d}{dz} cn\left(z|m\right) = -sn\left(z|m\right) \times dn\left(z|m\right), \tag{A2}$$

$$\frac{d}{dz} dn\left(z|m\right) = -m \times sn\left(z|m\right) \times cn\left(z|m\right). \tag{A3}$$

They also satisfy quadratic relations, such as

$$\left(sn\left(z|m\right)\right)^2 + \left(cn\left(z|m\right)\right)^2 = 1; \quad m\left(sn\left(z|m\right)\right)^2 + \left(dn\left(z|m\right)\right)^2 = 1. \tag{A4}$$

When m is a real number in the range $-\infty < m < 1$, the function $sn\left(z|m\right)$ oscillates between the values -1 to $+1$, similar to the trigonometric function $\sin\left(z\right)$, vanishing at $z \to 0$, and reaching a maximum at the quarter period $z = K\left(m\right)$, where $K\left(m\right)$ is the elliptic integral as a function of m. From the quadratic relations above, it is deduced that the behavior of $cn\left(z|m\right)$ is that it oscillates similar to a cosine $\cos\left(z\right)$, while $dn\left(z|m\right)$ oscillates between the positive values $+1$ and and $\left(1-m\right)^{1/2}$. When $m > 1$ the behavior is still oscillatory but quite different than $\sin\left(z\right)$, $\cos\left(z\right)$,etc.. However, it is possible to use identities to rewrite the solution in terms of $sn\left(z|m'\right), cn\left(z|m'\right), dn\left(z|m'\right)$ where $m' = 1-m$ is again in the range $-\infty < m' < 1$. We have used such identities so that all the m values that appear in our solutions below are in the range $-\infty < m < 1$. Then the reader can get a feeling of the behavior of the solutions by the analogy to trigonometric $\sin\left(z\right)$, $\cos\left(z\right)$,etc..

We begin with the $K = 0$ cases; there are five different regions for the remaining parameters as listed in Figs.(5-9)

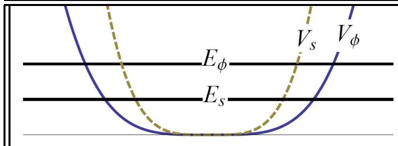

FIG. 5

$b < 0,\ c > 0,\ E_\phi \geq E_s > 0$

$$\phi = \left(\frac{E+\rho_r}{-4b}\right)^{1/4} \frac{sn(\frac{\tau+\delta}{T_\phi}|\frac{1}{2})}{dn(\frac{\tau+\delta}{T_\phi}|\frac{1}{2})},\ T_\phi = \left(-16b\left(E+\rho_r\right)\right)^{-1/4}$$

$$s = \left(\frac{E}{4c}\right)^{1/4} \frac{sn(\frac{\tau}{T_s}|\frac{1}{2})}{dn(\frac{\tau}{T_s}|\frac{1}{2})},\ T_s = (16Ec)^{-1/4}$$

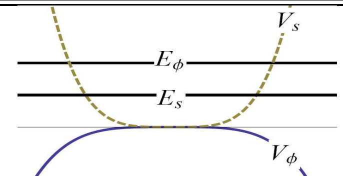

FIG. 6

$b > 0,\ c > 0,\ E_\phi \geq E_s > 0$

$$\phi = \left(\frac{E+\rho_r}{b}\right)^{1/4} \frac{sn\left(\frac{\tau+\delta}{T_\phi}|\frac{1}{2}\right)}{1+cn\left(\frac{\tau+\delta}{T_\phi}|\frac{1}{2}\right)},\ T_\phi = \frac{1}{\sqrt{2}}\left(16b\left(E+\rho_r\right)\right)^{-1/4}$$

$$s = \left(\frac{E}{4c}\right)^{1/4} \frac{sn(\frac{\tau}{T_s}|\frac{1}{2})}{dn(\frac{\tau}{T_s}|\frac{1}{2})},\ T_s = (16cE)^{-1/4}$$

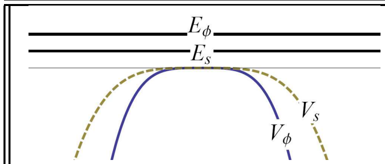

FIG. 7

$b > 0,\ c < 0,\ E_\phi \geq E_s > 0$

$$\phi = \left(\frac{E+\rho_r}{b}\right)^{1/4} \frac{sn\left(\frac{\tau+\delta}{T_\phi}|\frac{1}{2}\right)}{1+cn\left(\frac{\tau+\delta}{T_\phi}|\frac{1}{2}\right)},\ T_\phi = \frac{1}{\sqrt{2}}\left(16b\left(E+\rho_r\right)\right)^{-1/4}$$

$$s = \left(\frac{E}{-c}\right)^{1/4} \frac{sn\left(\frac{\tau}{T_s}|\frac{1}{2}\right)}{1+cn\left(\frac{\tau}{T_s}|\frac{1}{2}\right)},\ T_s = \frac{1}{\sqrt{2}}\left(-16cE\right)^{-1/4}$$

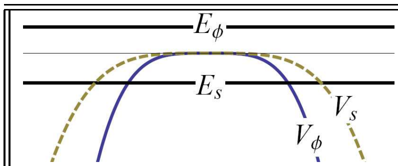

FIG. 8

$b > 0,\ c < 0,\ E_\phi \geq E_s$

$E_\phi > 0,\ E_s < 0$

$$\phi = \left(\frac{E+\rho_r}{b}\right)^{1/4} \frac{sn\left(\frac{\tau+\delta}{T_\phi}|\frac{1}{2}\right)}{1+cn\left(\frac{\tau+\delta}{T_\phi}|\frac{1}{2}\right)},\ T_\phi = \frac{1}{\sqrt{2}}\left(16b\left(E+\rho_r\right)\right)^{-1/4}$$

$$s = \left(\frac{E}{c}\right)^{1/4} \frac{1}{cn(\frac{\tau}{T_s}|\frac{1}{2})},\ T_s = (16cE)^{-1/4}$$

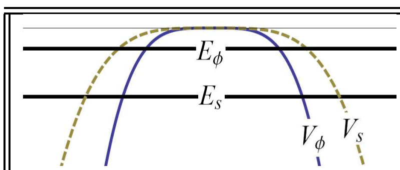

FIG. 9

$b > 0,\ c < 0,\ 0 > E_\phi \geq E_s$

$$\phi = \left(\frac{-(E+\rho_r)}{b}\right)^{1/4} \frac{1}{cn\left(\frac{\tau+\delta}{T_\phi}|\frac{1}{2}\right)},\ T_\phi = \left(-16b\left(E+\rho_r\right)\right)^{-1/4}$$

$$s = \left(\frac{E}{c}\right)^{1/4} \frac{1}{cn\left(\frac{\tau}{T_s}|\frac{1}{2}\right)},\ T_s = (16cE)^{-1/4}$$

Note that as the parameters $b, c, E, (E+\rho_r)$ change signs the corresponding solutions and physical behaviors change qualitatively. Nevertheless, the mathematical expressions in Figs.(5-9) are related to each other by the following rules for analytic continuation, where x is real

$$\left.\begin{array}{l} \frac{1}{\sqrt{2}} sn\left(\frac{e^{\pm i\pi/4}}{\sqrt{2}} x|\frac{1}{2}\right) = sn\left(x|\frac{1}{2}\right) \\ 1 + cn\left(\frac{e^{\pm i\pi/4}}{\sqrt{2}} x|\frac{1}{2}\right) = dn\left(x|\frac{1}{2}\right) \end{array}\right\}, \text{ relates } \begin{cases} \text{Figs.(6) to (5), } b \text{ flips sign} \\ \text{Figs.(7) to (6), } c \text{ flips sign} \end{cases} \tag{A5}$$

$$cn\left(xe^{\pm i\pi/4}|\frac{1}{2}\right) = \frac{1 + cn\left(\frac{x}{\sqrt{2}}|\frac{1}{2}\right)}{sn\left(\frac{x}{\sqrt{2}}|\frac{1}{2}\right)}, \text{ relates } \begin{cases} \text{Figs.(9) to (7), } E \text{ flips sign} \\ \text{Figs.(9) to (8), } (E+\rho) \text{ flips sign} \end{cases} \tag{A6}$$

So, it is possible to write a single formula to cover all the solutions (such as the formulas in Fig.9, modified with appropriate absolute signs)

$$\begin{array}{l} \phi(\tau) = \left|\frac{E+\rho_r}{b}\right|^{1/4} \left\{cn\left[\left(-16b\left(E+\rho_r\right)\right)^{1/4}(\tau+\delta) \ | \ \frac{1}{2}\right]\right\}^{-1}, \\ s(\tau) = \left|\frac{E}{c}\right|^{1/4} \left\{cn\left[\left(16cE\right)^{1/4}\tau \ | \ \frac{1}{2}\right]\right\}^{-1}, \end{array} \tag{A7}$$

and then analytically continue the argument of the Jacobi elliptic functions to obtain the other expressions. In this form all signs of the parameters $b, c, E, (E+\rho_r)$ are permitted, thus capturing the physical behavior of all corresponding regions of parameter space with a single expression (when $K=0$). Under these flips of signs the functions ϕ, s remain real even though the argument of the function is complex. This unified version is convenient to feed it to a computer to obtain plots of the solutions.

There is a similar analytic continuation for the cases with nonzero curvature given below, but the formulas for analytic continuation are considerably more involved, so we will not bother to discuss them.

Next we have the $K > 0$ cases, with eleven combinations which are listed in Figs.(10-19)

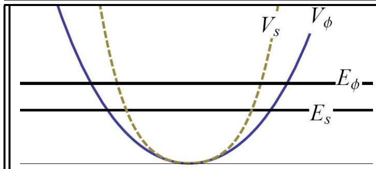

FIG. 10

$b < 0,\ c > 0, E_\phi \geq E_s > 0$

$$\phi = \sqrt{\frac{1-K^2T_\phi^4}{8|b|T_\phi^2}}\frac{sn(\frac{\tau+\delta}{T_\phi}|m_\phi)}{dn(\frac{\tau+\delta}{T_\phi}|m_\phi)},\quad m_\phi = \tfrac{1}{2}\left(1-KT_\phi^2\right) \leq \tfrac{1}{2},\quad T_\phi = \tfrac{1}{\sqrt{K}}\left(1-\tfrac{16b}{K^2}\left(E+\rho_r\right)\right)^{-1/4}$$

$$s = \sqrt{\frac{1-K^2T_s^4}{8cT_s^2}}\frac{sn(\frac{\tau}{T_s}|m_s)}{dn(\frac{\tau}{T_s}|m_s)},\quad m_s = \tfrac{1}{2}\left(1-KT_s^2\right) \leq \tfrac{1}{2},\quad T_s = \tfrac{1}{\sqrt{K}}\left(1+\tfrac{16Ec}{K^2}\right)^{-1/4}$$

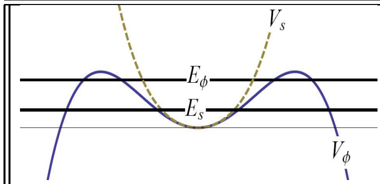

FIG. 11

$b > 0,\ c > 0, E_\phi \geq E_s > 0$

$E_\phi < \frac{K^2}{16b},\ |\phi(0)| < \sqrt{\frac{K}{4b}}$

$$\phi = \sqrt{\frac{KT_\phi^2-1}{2bT_\phi}}\,sn\left(\frac{\tau+\delta}{T_\phi}|m_\phi\right),\quad m_\phi = KT_\phi^2 - 1 \leq 1,\quad T_\phi = \tfrac{\sqrt{2}}{\sqrt{K}}\left(1+\sqrt{1-\tfrac{16b(E+\rho_r)}{K^2}}\right)^{-1/2}$$

$$s = \sqrt{\frac{1-K^2T_s^4}{8cT_s^2}}\frac{sn(\frac{\tau}{T_s}|m_s)}{dn(\frac{\tau}{T_s}|m_s)},\quad m_s = \tfrac{1}{2}\left(1-KT_s^2\right) \leq \tfrac{1}{2},\quad T_s = \tfrac{1}{\sqrt{K}}\left(1+\tfrac{16Ec}{K^2}\right)^{-1/4}$$

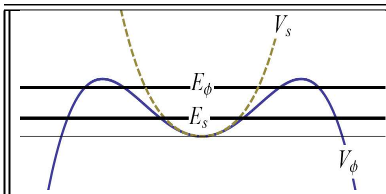

FIG. 12

$b > 0,\ c > 0, E_\phi \geq E_s > 0$

$E_\phi < \frac{K^2}{16b},\ |\phi(0)| > \sqrt{\frac{K}{4b}}$

$$\phi = \sqrt{\frac{KT_\phi^2+1}{4bT_\phi^2}}\frac{1}{cn\left(\frac{\tau+\delta}{T_\phi}|m_\phi\right)},\quad m_\phi = \tfrac{1}{2}\left(1-KT_\phi^2\right) \leq 0,\quad T_\phi = \tfrac{1}{\sqrt{K}}\left(1-\tfrac{16b}{K^2}\left(E+\rho_r\right)\right)^{-1/4}$$

$$s = \sqrt{\frac{1-K^2T_s^4}{8cT_s^2}}\frac{sn(\frac{\tau}{T_s}|m_s)}{dn(\frac{\tau}{T_s}|m_s)},\quad m_s = \tfrac{1}{2}\left(1-KT_s^2\right) \leq \tfrac{1}{2},\quad T_s = \left(K^2+16cE\right)^{-1/4}$$

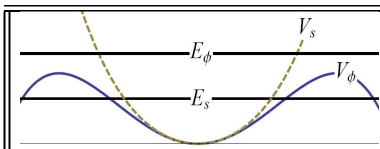

FIG. 13

$b > 0,\ c > 0,$

$E_\phi \geq E_s > 0,\ \ E_\phi > \frac{K^2}{16b}$

$$\phi(\tau) = \left(\frac{E+\rho_r}{b}\right)^{1/4}\frac{sn\left(\frac{\tau+\delta}{T_\phi}|m_\phi\right)}{1+cn\left(\frac{\tau+\delta}{T_\phi}|m_\phi\right)},\quad m_\phi = \tfrac{1}{2} + KT_\phi^2 \leq 1,\quad T_\phi = \left(64b\left(E+\rho_r\right)\right)^{-1/4}$$

$$s(\tau) = \sqrt{\frac{1-K^2T_s^4}{8cT_s^2}}\frac{sn(\frac{\tau}{T_s}|m_s)}{dn(\frac{\tau}{T_s}|m_s)},\quad m_s = \tfrac{1}{2}\left(1-KT_s^2\right) \leq \tfrac{1}{2},\quad T_s = \left(K^2+16cE\right)^{-1/4}$$

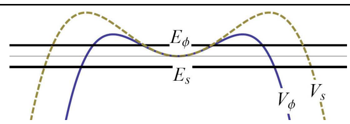

FIG. 14

$b > 0,\ c < 0,$

$E_s \leq 0 \leq E_\phi < \frac{K^2}{16b}$

$|\phi(0)| > \sqrt{\frac{K}{4b}}, |s(0)| > \sqrt{\frac{K}{4|c|}}$

$$\phi = \sqrt{\frac{KT_\phi^2+1}{4bT_\phi^2}}\frac{1}{cn\left(\frac{\tau+\delta}{T_\phi}|m_\phi\right)},\quad m_\phi = \frac{1}{2}\left(1-KT_\phi^2\right) \leq 0,\quad T_\phi = \left(K^2 - 16b\left(E+\rho_r\right)\right)^{-1/4}$$

$$s = \sqrt{\frac{KT_s^2+1}{4|c|T_s^2}}\frac{1}{cn\left(\frac{\tau}{T_s}|m_s\right)},\quad m_s = \frac{1}{2}\left(1-KT_s^2\right) \leq \frac{1}{2},\quad T_s = \left(K^2 + 16\left|c\right|\left|E\right|\right)^{-1/4}$$

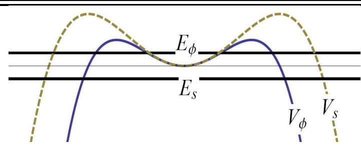

FIG. 15

$b > 0,\ c < 0,$

$E_\phi \geq E_s,\ E_\phi < \frac{K^2}{16b},$

$|\phi(0)| < \sqrt{\frac{K}{4b}}, |s(0)| > \sqrt{\frac{K}{4|c|}}$

$$\phi = \sqrt{\frac{KT_\phi^2-1}{2bT_\phi}}sn\left(\frac{\tau+\delta}{T_\phi}|m_\phi\right),\quad m_\phi = KT_\phi^2 - 1 \leq 1,\quad T_\phi = \left(\frac{K}{2} + \sqrt{\frac{K^2}{4} - 4b\left(E+\rho_r\right)}\right)^{-\frac{1}{2}}$$

$$s = \sqrt{\frac{KT_s^2+1}{4|c|T_s^2}}\frac{1}{cn\left(\frac{\tau}{T_s}|m_s\right)},\quad m_s = \frac{1}{2}\left(1-KT_s^2\right) \leq \frac{1}{2},\quad T_s = \left(K^2 - 16\left|c\right|E\right)^{-1/4}$$

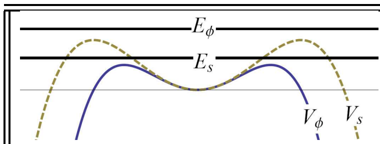

FIG. 16

$b > 0,\ c < 0,\ E_\phi \geq E_s$

$E_\phi > \frac{K^2}{16b},\ E_s < \frac{K^2}{16|c|}$

$|s(0)| > \sqrt{\frac{K}{4|c|}}$

$$\phi(\tau) = \left(\frac{E+\rho_r}{b}\right)^{1/4}\frac{sn\left(\frac{\tau+\delta}{T_\phi}|m_\phi\right)}{1+cn\left(\frac{\tau+\delta}{T_\phi}|m_\phi\right)},\quad m_\phi = \frac{1}{2} + KT_\phi^2 \leq 1,\quad T_\phi = \left(64b\left(E+\rho_r\right)\right)^{-1/4}$$

$$s(\tau) = \sqrt{\frac{KT_s^2+1}{4|c|T_s^2}}\frac{1}{cn\left(\frac{\tau}{T_s}|m_s\right)},\quad m_s = \frac{1}{2}\left(1-KT_s^2\right) \leq 0,\quad T_s = \left(K^2 - 16\left|c\right|E\right)^{-1/4}$$

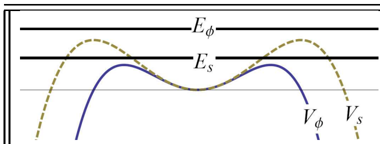

FIG. 17

$b > 0,\ c < 0,\ E_\phi \geq E_s$

$E_\phi > \frac{K^2}{16b},\ 0 < E_s < \frac{K^2}{16|c|}$

$|s(0)| < \sqrt{\frac{K}{4|c|}}$

$$\phi = \left(\frac{E+\rho_r}{b}\right)^{1/4}\frac{sn\left(\frac{\tau+\delta}{T_\phi}|m_\phi\right)}{1+cn\left(\frac{\tau+\delta}{T_\phi}|m_\phi\right)},\quad m_\phi = \frac{1}{2} + KT_\phi^2 \leq 1,\quad T_\phi = \left(64b\left(E+\rho_r\right)\right)^{-1/4}$$

$$s = \frac{\sqrt{KT_s^2-1}}{\sqrt{2|c|T_s}}sn\left(\frac{\tau}{T_s}|m_s\right),\quad m_s = KT_s^2 - 1 \leq 1,\quad T_s = \left(\frac{K}{2} + \sqrt{\frac{K^2}{4} - 4\left|c\right|E}\right)^{-1/2}$$

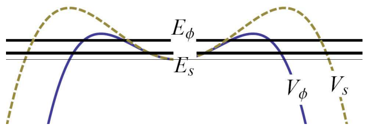

FIG. 18

$b>0,\ c<0,$

$E_\phi \geq E_s > 0,\ E_\phi < \frac{K^2}{16b},$

$|\phi(0)| > \sqrt{\frac{K}{4b}}, |s(0)| < \sqrt{\frac{K}{4b}}$

$$\phi = \sqrt{\frac{KT_\phi^2+1}{4bT_\phi^2}}\frac{1}{cn\left(\frac{\tau+\delta}{T_\phi}|m_\phi\right)}, \quad m_\phi = \frac{1}{2}\left(1-KT_\phi^2\right) \leq 0, \quad T_\phi = \left(K^2 - 16b\left(E+\rho_r\right)\right)^{-1/4}$$

$$s = \frac{\sqrt{KT_s^2-1}}{\sqrt{2|c|T_s}} sn\left(\frac{\tau}{T_s}|m_s\right), \quad m_s = KT_s^2 - 1 \leq 1, \quad T_s = \left(\frac{K}{2}+\sqrt{\frac{K^2}{4}-4|c|E}\right)^{-1/2}$$

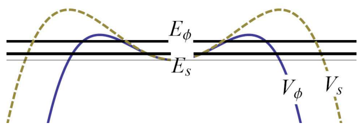

FIG. 19

$b>0,\ c<0,$

$E_\phi \geq E_s,\ 0 < E_\phi < \frac{K^2}{16b},$

$|\phi(0)| < \sqrt{\frac{K}{4b}}, |s(0)| < \sqrt{\frac{K}{4|c|}}$

$$\phi = \sqrt{\frac{KT_\phi^2-1}{2bT_\phi}} sn\left(\frac{\tau+\delta}{T_\phi}|m_\phi\right), \quad m_\phi = KT_\phi^2 - 1 \leq 1, \quad T_\phi = \left(\frac{K}{2}+\sqrt{\frac{K^2}{4}-4b\left(E+\rho_r\right)}\right)^{-\frac{1}{2}}$$

$$s = \sqrt{\frac{KT_s^2-1}{2|c|T_s}} sn\left(\frac{\tau}{T_s}|m_s\right), \quad m_s = KT_s^2 - 1 \leq 1, \quad T_s = \left(\frac{K}{2}+\sqrt{\frac{K^2}{4}-4|c|E}\right)^{-1/2}$$

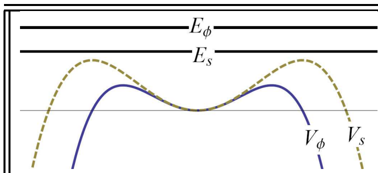

FIG. 20

$b>0,\ c<0,$

$E_\phi \geq E_s,\ E_s > \frac{K^2}{16|c|}$

$$\phi = \left(\frac{E+\rho_r}{b}\right)^{1/4} \frac{sn\left(\frac{\tau+\delta}{T_\phi}|m_\phi\right)}{1+cn\left(\frac{\tau+\delta}{T_\phi}|m_\phi\right)}, \quad m_\phi = \frac{1}{2}+KT_\phi^2 \leq 1, \quad T_\phi = \left(64b\left(E+\rho_r\right)\right)^{-1/4}$$

$$s = \left(\frac{E}{|c|}\right)^{1/4} \frac{sn\left(\frac{\tau}{T_s}|m_s\right)}{1+cn\left(\frac{\tau}{T_s}|m_s\right)}, \quad m_s = \frac{1}{2}+KT_s^2 \leq 1, \quad T_s = \left(64|c|E\right)^{-1/4}$$

Finally, for $K<0$ there are nine combinations which are listed in Figs.(21-29)

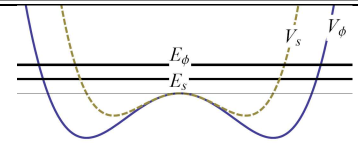

FIG. 21

$b<0,\ c>0,\ E_\phi \geq E_s > 0$

$$\phi = \sqrt{\frac{1-K^2T_\phi^4}{8|b|T_\phi^2}}\frac{sn\left(\frac{\tau+\delta}{T_\phi}|m_\phi\right)}{dn\left(\frac{\tau+\delta}{T_\phi}|m_\phi\right)},\quad m_\phi = \frac{1}{2}\left(1+|K|\,T_\phi^2\right) \leq 1,\quad T_\phi = \left(K^2+16\,|b|\,(E+\rho_r)\right)^{-1/4}$$

$$s = \sqrt{\frac{1-K^2T_s^4}{8cT_s^2}}\frac{sn\left(\frac{\tau}{T_s}|m_s\right)}{dn\left(\frac{\tau}{T_s}|m_s\right)},\quad m_s = \frac{1}{2}\left(1+|K|\,T_s^2\right) \leq 1,\quad T_s = \left(K^2+16cE\right)^{-1/4}$$

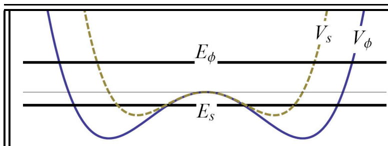

FIG. 22

$b<0,\ c>0,$

$\frac{-K^2}{16c} \leq E_s \leq 0 \leq E_\phi$

$$\phi = \sqrt{\frac{1-K^2T_\phi^4}{8|b|T_\phi^2}}\frac{sn\left(\frac{\tau+\delta}{T_\phi}|m_\phi\right)}{dn\left(\frac{\tau+\delta}{T_\phi}|m_\phi\right)},\quad m_\phi = \frac{1}{2}\left(1+|K|\,T_\phi^2\right) \leq 1,\quad T_\phi = \left(K^2+16\,|b|\,(E+\rho_r)\right)^{-1/4}$$

$$s = \pm\sqrt{\frac{|K|T_s^2-1}{4cT_s^2}}dn\left(\frac{\tau}{T_s}|m_s\right),\quad m_s = \left(2-\frac{1}{2}\,|K|\,T_s^2\right) \leq 1,\quad T_s = 2\left(|K|+\left(K^2-16c\,|E|\right)^{1/2}\right)^{-1/2}$$

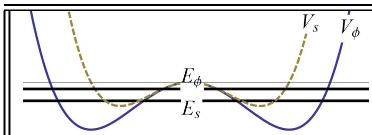

FIG. 23

$b<0,\ c>0,$

$\frac{-K^2}{16c} \leq E_s \leq E_\phi \leq 0$

$$\phi = \pm\sqrt{\frac{|K|T_\phi^2-1}{4|b|T_\phi^2}}dn\left(\frac{\tau}{T_\phi}|m_\phi\right),\quad m_\phi = \left(2-\frac{1}{2}\,|K|\,T_\phi^2\right) \leq 1,\quad T_\phi = 2\left(|K|+\sqrt{K^2-16\,|b|\,|E+\rho_r|}\right)^{-1/2}$$

$$s = \pm\sqrt{\frac{|K|T_s^2-1}{4cT_s^2}}dn\left(\frac{\tau}{T_s}|m_s\right),\quad m_s = \left(2-\frac{1}{2}\,|K|\,T_s^2\right) \leq 1,\quad T_s = 2\left(|K|+\sqrt{K^2-16c\,|E|}\right)^{-1/2}$$

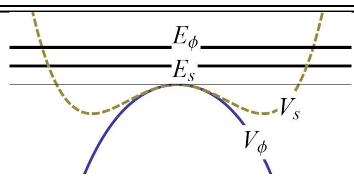

FIG. 24

$b>0,\ c>0,\ E_\phi \geq E_s > 0$

$$\phi = \sqrt{\frac{1}{8bT_\phi^2}}\frac{sn\left(\frac{\tau+\delta}{T_\phi}|m_\phi\right)}{1+cn\left(\frac{\tau+\delta}{T_\phi}|m_\phi\right)},\quad m_\phi = \frac{1}{2}-|K|\,T_\phi^2 \leq \frac{1}{2},\quad T_\phi = \left(64b\,(E+\rho_r)\right)^{-1/4}$$

$$s = \sqrt{\frac{1-K^2T_s^4}{8cT_s^2}}\frac{sn\left(\frac{\tau}{T_s}|m_s\right)}{dn\left(\frac{\tau}{T_s}|m_s\right)},\quad m_s = \frac{1}{2}\left(1+|K|\,T_s^2\right) \leq 1,\quad T_s = \left(K^2+16cE\right)^{-1/4}$$

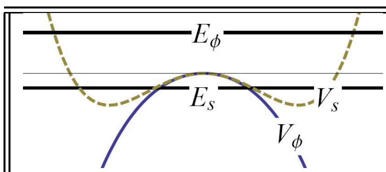

FIG. 25

$b>0,\ c>0,\ E_\phi > E_s$

$E_\phi > 0,\ 0 > E_s > \frac{-K^2}{16c}$

$$\phi = \left(\frac{-|E|+\rho_r}{b}\right)^{1/4}\frac{sn\left(\frac{\tau+\delta}{T_\phi}|m_\phi\right)}{1+cn\left(\frac{\tau+\delta}{T_\phi}|m_\phi\right)},\quad m_\phi = \frac{1}{2}-|K|\,T_\phi^2 \leq \frac{1}{2},\quad T_\phi = \left(64b\,(E+\rho_r)\right)^{-1/4}$$

$$s = \pm\sqrt{\frac{|K|T_s^2-1}{4cT_s^2}}dn\left(\frac{\tau}{T_s}|m_s\right),\quad m_s = \left(2-\frac{1}{2}\,|K|\,T_s^2\right) \leq 1,\quad T_s = 2\left(|K|+\sqrt{K^2-16c\,|E|}\right)^{-1/2}$$

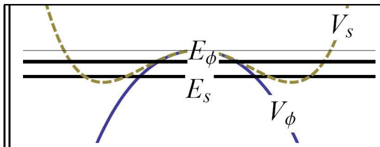

FIG. 26

$b > 0,\ c > 0,$

$0 > E_\phi \geq E_s > \frac{-K^2}{16c}$

$$\phi = \sqrt{\frac{1-|K|T_\phi^2}{4bT_\phi^2}}\frac{1}{cn\left(\frac{\tau+\delta}{T_\phi}|m_\phi\right)},\quad m_\phi = \tfrac{1}{2}\left(1+|K|\,T_\phi^2\right) \leq 1,\quad T_\phi = \left(K^2+16b\,|E+\rho_r|\right)^{-1/4}$$

$$s = \pm\sqrt{\frac{|K|T_s^2-1}{4cT_s^2}}dn\left(\frac{\tau}{T_s}|m_s\right),\quad m_s = \left(2-\tfrac{1}{2}\,|K|\,T_s^2\right) \leq 1,\quad T_s = 2\left(|K|+\sqrt{K^2-16c\,|E|}\right)^{-1/2}$$

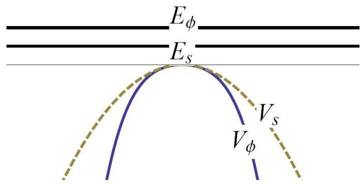

FIG. 27

$b > 0,\ c < 0,\ E_\phi \geq E_s > 0$

$$\phi = \left(\frac{E+\rho_r}{b}\right)^{1/4}\frac{sn\left(\frac{\tau+\delta}{T_\phi}|m_\phi\right)}{1+cn\left(\frac{\tau+\delta}{T_\phi}|m_\phi\right)},\quad m_\phi = \tfrac{1}{2}-|K|\,T_\phi^2 \leq \tfrac{1}{2},\quad T_\phi = \left(64b\left(E+\rho_r\right)\right)^{-1/4}$$

$$s = \left(\frac{E}{|c|}\right)^{1/4}\frac{sn\left(\frac{\tau}{T_s}|m_s\right)}{1+cn\left(\frac{\tau}{T_s}|m_s\right)},\quad m_s = \tfrac{1}{2}-|K|\,T_s^2 \leq \tfrac{1}{2},\quad T_s = \left(64\,|c|\,E\right)^{-1/4}$$

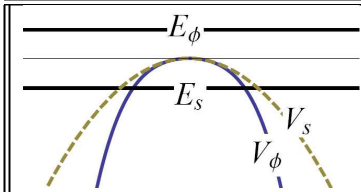

FIG. 28

$b > 0,\ c < 0,\ E_\phi > E_s$

$E_\phi > 0,\ E_s < 0$

$$\phi = \sqrt{\frac{1}{8bT_\phi^2}}\frac{sn\left(\frac{\tau+\delta}{T_\phi}|m_\phi\right)}{1+cn\left(\frac{\tau+\delta}{T_\phi}|m_\phi\right)},\quad m_\phi = \tfrac{1}{2}-|K|\,T_\phi^2 \leq \tfrac{1}{2},\quad T_\phi = \left(64b\left(E+\rho_r\right)\right)^{-1/4}$$

$$s = \sqrt{\frac{1-|K|T_s^2}{4|c|T_s^2}}\frac{1}{cn\left(\frac{\tau}{T_s}|m_s\right)},\quad m_s = \tfrac{1}{2}\left(1+|K|\,T_s^2\right) \leq 1,\quad T_s = \left(K^2+16\,|c|\,|E|\right)^{-1/4}$$

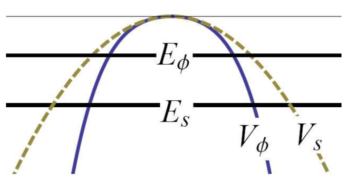

FIG. 29

$b > 0,\ c < 0,\ 0 > E_\phi \geq E_s$

$$\phi = \sqrt{\frac{1-|K|T_\phi^2}{4b}}\frac{1}{cn\left(\frac{\tau+\delta}{T_\phi}|m_\phi\right)},\quad m_\phi = \tfrac{1}{2}\left(1+|K|\,T_\phi^2\right) \leq 1,\quad T_\phi = \left(K^2+16b\,|E+\rho_r|\right)^{-1/4}$$

$$s = \sqrt{\frac{1-|K|T_s^2}{4|c|}}\frac{1}{cn\left(\frac{\tau}{T_s}|m_s\right)},\quad m_s = \tfrac{1}{2}\left(1+|K|\,T_s^2\right) \leq 1,\quad T_s = \left(K^2+16\,|c|\,|E|\right)^{-1/4}$$

[1] A. H. Guth, Phys. Rev. D **23**, 347 (1981).

[2] A. D. Linde, Phys. Lett. B **108**, 389 (1982).

[3] A. Albrecht, P. J. Steinhardt, Phys. Rev. Lett. **48**, 1220 (1982).

[4] C. Mathiazhagan and V. B. Johri, Class. Quantum Grav. **1**, L 29 (1984).

[5] D. La and P. J. Steinhardt, Phys. Rev. D **62**, 376 (1989).

[6] F. Accetta and P. J. Steinhardt, Phys. Rev. Lett. **32**, 2740 (1990).

[7] A. Linde, Phys. Lett. B**238**, 160 (1990).

[8] J. Khoury, B. A. Ovrut, P. J. Steinhardt and N. Turok, Phys. Rev. D 64, 123522 (2001) [arXiv:hep-th/0103239].

[9] J. K. Erickson, D. H. Wesley, P. J. Steinhardt and N. Turok, Phys. Rev. D 69, 063514 (2004) [arXiv:hep-th/0312009].

[10] D. Bessada, W.H. Kinney, D. Stojkovic and J. Wang, Phys. Rev. D. 81, 042510 (2010).

[11] A. G. Riess *et al.* [Supernova Search Team Collaboration], Astron. J. **116**, 1009 (1998); S. Perlmutter *et al.* [Supernova Cosmology Project Collaboration], Astrophys. J. **517**, 565 (1999); C. L. Bennett *et al.*, Astrophys. J. Suppl. **148**, 1 (2003); M. Tegmark *et al.* [SDSS Collaboration], Phys. Rev. D **69**, 103501 (2004); S. W. Allen, *et al.*, Mon. Not. Roy. Astron. Soc. **353**, 457 (2004).

[12] B. Ratra and P. J. E. Peebles, Phys. Rev. D **37**, 3406 (1988); C. Wetterich, Nucl. Phys. B **302**, 668 (1988); R.R. Caldwell, R. Dave, and P.J. Steinhardt, Phys. Rev. Lett. **80**, 1582 (1998). A. R. Liddle and R. J. Scherrer, Phys. Rev. D **59**, 023509 (1999); I. Zlatev, L. M. Wang and P. J. Steinhardt, Phys. Rev. Lett. **82**, 896 (1999); Z. K. Guo, N. Ohta and Y. Z. Zhang, Mod. Phys. Lett. A **22**, 883 (2007); D. Stojkovic, G.D. Starkman and R. Matsuo, Phys. Rev D 77, 063006 (2008); E. Greenwood, E. Halstead, R. Poltis, and D. Stojkovic, Phys. Rev. D 79, 103003 (2009); S. Dutta and R. J. Scherrer, Phys. Rev. D **78**, 123525 (2008); S. Dutta and R. J. Scherrer, Phys. Rev. D **78**, 083512 (2008); D. C. Dai, S. Dutta and D. Stojkovic, Phys. Rev. D **80**, 063522 (2009); S. Dutta, S. D. H. Hsu, D. Reeb and R. J. Scherrer, Phys. Rev. D **79**, 103504 (2009); S. Dutta, E. N. Saridakis and R. J. Scherrer, Phys. Rev. D **79**, 103005 (2009); S. Dutta and R. J. Scherrer, Phys. Lett. B **676**, 12 (2009).

[13] K. Maeda, Phys. Rev. D**39**, 3159 (1989).

[14] I. Bars and S-H. Chen, “The Big Bang and Inflation United by an Analytic Solution”, Phys. Rev. **D83** (2011) 043522 [arXiv:1004.0752v2].

[15] I. Bars, S-H. Chen and N. Turok, “Geodesically Complete Analytic Solutions for a Cyclic Universe.”, Phys.Rev. D84 (2011) 083513 [arXiv:1105.3606].

[16] I. Bars, “Geodesically Complete Universe”, arXiv:1109.5872 [gr-qc].

[17] I. Bars, S. H. Chen, P. J. Steinhardt, N. Turok, “Antigravity and the Big Crunch/Big Bang Transition”, [arXiv:1112.2470]

[18] I. Bars, S. H. Chen, P. J. Steinhardt, N. Turok, in preparation.

[19] For a recent summary and status of 2T-physics, see I. Bars, “Gauge Symmetry in Phase Space, Consequences for Physics and Spacetime”, Int. J. Mod. Phys. **A25** (2010) 5235 [arXiv:1004.0668 [hep-th]].

[20] I. Bars, ”Gravity in 2T-Physics”, Phys. Rev. **D77** (2008) 125027 [arXiv:0804.1585[tep-th]].

[21] I. Bars, S. H. Chen ”Geometry and Symmetry Structures in 2T Gravity”, Phys. Rev. **D79** (2009) 085021 [arXiv:0811.2510v2 [hep-th]].

[22] P. Hořava and E.Witten, Nucl. Phys. **B460** (1996) 506 [arXiv:hep-th/9510209; hep-th/9603142].

[23] L. Randall and R. Sundrum, Phys. Rev. Lett. **83** (1999) 4690; ibid. **83** (1999) 3370.

[24] J. Khoury, B. A. Ovrut, N. Seiberg, P. J. Steinhardt, N. Turok, Phys.Rev. D65 (2002) 086007 [arXiv:hep-th/0108187].

[25] P. McFadden and N. Turok, “Conformal Symmetry of Brane World Effective Actions”, Phys. Rev. **D71** (2005) 021901 [arXiv:hep-th/0409122].

[26] G. tHooft. Lecture in conference, *Conformal Nature of the Universe*, see http://www.pirsa.org/C12027 .

[27] I. Bars, ”The Standard Model of Particles and Forces in the Framework of 2T-physics”, Phys.Rev. D74 (2006) 085019 [hep-th/0606045].

[28] I. Bars, talk at http://pirsa.org/12050077/, also paper in preparation.

[29] M. Abramowitz, I.A. Stegun, ”*Handbook of Mathematical Functions*”, Dover (1965), ISBN 0486612724.

[30] I. Bars, Phys. Rev. D79 (2009)045009 [arXiv:hep-th/0810.2075]

[31] I. Bars, [arXiv:gr-qc1109.5872]

[32] S. Weinberg, *The Quantum Theory of Fields*, Volume III, Cambridge 2000.

[33] B. de Wit and A. Van Proeyen, “Potentials and Symmetries of General Gauged $\mathcal{N}$=2 Supergravity: Yang-Mills Models”, Nucl.Phys. **B245** (1984) 89.